

A Generalized Gaussian Process Model for Computer Experiments with Binary Time Series

Chih-Li Sung^a ¹, Ying Hung^b ¹, William Rittase^c, Cheng Zhu^c,
C. F. J. Wu^a ²

^aSchool of Industrial and Systems Engineering, Georgia Institute of Technology

^bDepartment of Statistics, Rutgers, the State University of New Jersey

^cDepartment of Biomedical Engineering, Georgia Institute of Technology

Abstract

Non-Gaussian observations such as binary responses are common in some computer experiments. Motivated by the analysis of a class of cell adhesion experiments, we introduce a generalized Gaussian process model for binary responses, which shares some common features with standard GP models. In addition, the proposed model incorporates a flexible mean function that can capture different types of time series structures. Asymptotic properties of the estimators are derived, and an optimal predictor as well as its predictive distribution are constructed. Their performance is examined via two simulation studies. The methodology is applied to study two different cell adhesion mechanisms, which were conducted by computer simulations. The fitted models reveal important biological differences between the two mechanisms in repeated bindings, which cannot be directly observed experimentally.

Keywords: Computer experiment, Gaussian process model, Single molecule experiment, Uncertainty quantification

¹Joint first authors.

²Corresponding author.

1 Introduction

Cell adhesion plays an important role in many physiological and pathological processes. This research is motivated by the analysis of a class of cell adhesion experiments called micropipette adhesion frequency assays, which is a method for measuring the kinetic rates between molecules in their native membrane environment. In a micropipette adhesion frequency assay, a red blood coated in a specific ligand is brought into contact with cell containing the native receptor for a predetermined duration, then retracted. The output of interest is binary, indicating whether a controlled contact results in adhesion. If there is an adhesion between molecules at the end of contact, retraction will stretch the red cell. If no adhesion resulted, the red cell will not be stretched. The kinetics of the molecular interaction can be derived through many repeated trials. In theory, these contacts should be independent Bernoulli trials. However, that there is a memory effect in the repeated tests and the quantification of such a memory effect is scientifically important (Zarnitsyna et al., 2007; Hung et al., 2008).

A cost-effective way to study the repeated adhesion frequency assays is through computer experiments, which study real systems using complex mathematical models and numerical tools like finite element analysis (Santner et al., 2003). They have been widely used as alternatives to physical experiments or observations, especially for the study of complex systems. For cell adhesion, performing physical experiments (i.e., lab work) is time-consuming and often involves complicated experimental manipulation. Therefore, instead of performing the actual lab work, computer simulations of mathematical models provide an efficient way to examine the complex mechanisms behind the adhesion.

Computer experiments, while cheaper compared with physical experiments, can often have long run times. Typically they are deterministic in the sense that the same input

produces the same output. Therefore, it is desirable to build an interpolator for the computer experiment outputs and use it as an “emulator” or “surrogate model” to predict results at untried input settings (Sacks et al., 1989; Santner et al., 2003). As a result, Gaussian process models whose predictors have the interpolation property are widely used as emulators for the analysis of computer experiments. Apart from the interpolation property, GP is popular for modeling complex systems because it can accommodate nonlinearity. The applications of GP can be found in many fields in science and engineering.

The conventional GP models are developed for continuous outputs with a Gaussian assumption, which does not hold in some scientific studies. For example, the focus of the cell adhesion frequency assays is to elicit the relationship between the setting of kinetic parameters/covariates and the adhesion score, which is binary. For binary outputs, the Gaussian assumption is not valid and GP models cannot be directly applied. Binary responses are common in computer experiments, but the extensions of GP models to non-Gaussian cases have received scant attention in computer experiment literature. Although there are intensive studies of generalized GP models for non-Gaussian data in machine learning and spatial statistics, such as Williams and Barber (1998), Zhang (2002), Rasmussen and Williams (2006), Nickisch and Rasmussen (2008) and Wang and Shi (2014), the asymptotic properties of estimators have not been systematically studied. Moreover, an analogy to the GP predictive distribution for binary data is important for uncertainty quantification in computer experiments, which has not yet been developed to the best of our knowledge.

Apart from the non-Gaussian responses, analysis of the repeated cell adhesion frequency assays poses another challenge, namely, how to incorporate a time series structure with complex interaction effects. It was discovered that cells appear to have the ability to remember the previous adhesion events and such a memory has an impact on the future adhesion behaviors (Zarnitsyna et al., 2007; Hung et al., 2008). The quantification of the

memory effect and how it interacts with the settings of the kinetic parameters in the binary time series are important but cannot be obtained by direct application of the conventional GP models. To consider the time series structure, a common practice is to construct a spatial-temporal model. However, a separable correlation function (e.g., Gelfand et al. (2004); Conti and O'Hagan (2010)) in which space and time are assumed to be independent is often implemented as a convenient way to address the computational issue. As a result, the estimation of interaction between space and time, which is of major interest here, is not allowed for. Even in the cases where nonseparable correlation functions (e.g., Gelfand et al. (2004); Fricker et al. (2013)) are implemented, the interaction effect is still not easily interpretable. Therefore, a new model that can model binary time series and capture interaction effects is called for.

To overcome the aforementioned limitations, we introduce a new class of models in this article. The idea is to generalize GP models to non-Gaussian responses and incorporate a flexible mean function that can estimate the time series structure and its interaction with the input variables. In particular, we focus on binary responses and introduce a new model which is analogous to the GP model with an optimal interpolating predictor. Rigorous studies of estimation, prediction, and inference are required for the proposed model and the derivations are complicated by the nature of binary response and the dependency of time series. By incorporating the time series structure, the proposed model can be applied to the analysis of repeated measurements with serial correlations beyond computer experiments. For example, it can be used for the analysis of non-Gaussian functional data which are common in longitudinal data analysis.

The remainder of this article is organized as follows. The new class of models is discussed in Section 2. In Section 3, asymptotic properties of the estimators are derived and the predictive distributions are constructed. Finite sample performance is demonstrated

by simulations in Section 4. In Section 5, the proposed method is illustrated with the analysis of computer experiments for cell adhesion frequency assays. Concluding remarks are given in Section 6. Mathematical proofs and algorithms are provided in Appendices. An implementation for our method can be found in `binaryGP` (Sung, 2017) in `R` (R Core Team, 2015).

2 Model

2.1 Generalized Gaussian process models for binary response

We first introduce a model for binary responses in computer experiments which is analogous to the conventional GP models for continuous outputs. Suppose a computer experiment has a d -dimensional input setting $\mathbf{x} = (x_1, \dots, x_d)'$ and for each setting the binary output is denoted by $y(\mathbf{x})$. Using a logistic link function, the Gaussian process model for binary data can be written as

$$\text{logit}(p(\mathbf{x})) = \alpha_0 + \mathbf{x}'\boldsymbol{\alpha} + Z(\mathbf{x}), \quad (1)$$

where $p(\mathbf{x}) = \mathbb{E}[y_t(\mathbf{x})]$, α_0 and $\boldsymbol{\alpha} = (\alpha_1, \dots, \alpha_d)'$ are the intercept and linear effects of the mean function of $p(\mathbf{x})$, and $Z(\cdot)$ is a zero mean Gaussian process with variance σ^2 , correlation function $R_{\boldsymbol{\theta}}(\cdot, \cdot)$, and unknown correlation parameters $\boldsymbol{\theta}$.

Various choices of correlation functions have been discussed in the literature. For example, the *power exponential correlation function* is commonly used in the analysis of computer experiments (Santner et al., 2003):

$$R_{\boldsymbol{\theta}}(\mathbf{x}_i, \mathbf{x}_j) = \exp \left\{ - \sum_{l=1}^d \frac{(x_{il} - x_{jl})^p}{\theta_l} \right\}, \quad (2)$$

where $\boldsymbol{\theta} = (\theta_1, \dots, \theta_d)$, the power p controls the smoothness of the output surface, and the parameter θ_l controls the decay of correlation with respect to the distance between x_{il} and x_{jl} . Recent studies have shown that a careful selection of the correlation function, such as orthogonal Gaussian processes proposed by Plumlee and Joseph (2018), can resolve the identifiability issue in the estimation of Gaussian process models (Hodges and Reich, 2010; Paciorek, 2010; Tuo and Wu, 2015). This is particularly important in the application of calibration problems where the parameter estimation plays a significant role. Depending on the objectives of the studies, different correlation functions can be incorporated into the proposed model and the theoretical results developed herein remain valid.

Similar extensions of GP models to binary outputs have been applied in many different fields. For example when \mathbf{x} represents a two-dimensional spatial domain, (1) becomes the spatial generalized linear mixed model proposed by Zhang (2002). In a Bayesian framework, Gaussian process priors are implemented for classification problems, such as in Williams and Barber (1998) and Gramacy and Polson (2011). Despite successful applications of these models, theoretical studies on the estimation and prediction properties are not available. Therefore, one focus of this paper is to provide theoretical supports for the estimation and prediction in (1).

2.2 Generalized Gaussian process models for binary time series

In this section, we introduce a new model for the analysis of computer experiments with binary time series, which is an extension of (1) that takes serial correlations between binary observations into account. Suppose for each setting of a computer experiment, a sequence of *binary time series* outputs $\{y_t(\mathbf{x})\}_{t=1}^T$ is generated. A generalized Gaussian process model

for binary time series can be written as:

$$\text{logit}(p_t(\mathbf{x})) = \eta_t(\mathbf{x}) = \sum_{r=1}^R \varphi_r y_{t-r}(\mathbf{x}) + \alpha_0 + \mathbf{x}'\boldsymbol{\alpha} + \sum_{l=1}^L \boldsymbol{\gamma}_l \mathbf{x} y_{t-l}(\mathbf{x}) + Z_t(\mathbf{x}), \quad (3)$$

where $p_t(\mathbf{x}) = \mathbb{E}[y_t(\mathbf{x})|H_t]$ is the conditional mean given the previous information $H_t = \{y_{t-1}(\mathbf{x}), y_{t-2}(\mathbf{x}), \dots\}$ and Z_t is assumed to vary independently over time. In model (3), $\{\varphi_r\}_{r=1}^R$ represents an autoregressive (AR) process with order R , and $\boldsymbol{\alpha} = (\alpha_1, \dots, \alpha_d)'$ represents the effects of \mathbf{x} , and $\{\boldsymbol{\gamma}_l\}_{l=1}^L$, where $\boldsymbol{\gamma}_l$ is a d -dimensional vector and represents the interaction between the input and the past outputs, which provides the flexibility of modeling different time series structures with different inputs. Without the Gaussian process assumption in (3), the mean function is closely related to the Zeger-Qaqish (1988) model and its extension in Hung et al. (2008) which take into account the autoregressive predictors in logistic regression.

Model (3) extends the applications of conventional GP to binary time series generated from computer experiments. The model is intuitively appealing; however, the issues of estimation, prediction, and inference are not straightforward due to the nature of binary response and the dependency structure.

3 Inference

Since model (1) can be written as a special case of model (3) when $R = 0, L = 0$ and $T = 1$, derivations herein are mainly based on model (3) with additional discussions given for (1) when necessary.

3.1 Estimation

Given n input settings $\mathbf{x}_1, \dots, \mathbf{x}_n$ in a computer experiment, denote $y_{it} \equiv y_t(\mathbf{x}_i)$ as the binary output generated from input \mathbf{x}_i at time t , where $\mathbf{x}_i \in \mathbb{R}^d$, $i = 1, \dots, n$, and $t = 1, \dots, T$. Let N be the total number of the outputs, i.e., $N = nT$. In addition, at each time t , denote \mathbf{y}_t as an n -dimensional vector $\mathbf{y}_t = (y_{1t}, \dots, y_{nt})'$ with conditional mean $\mathbf{p}_t = (p_{1t}, \dots, p_{nt})'$, where $p_{it} = \mathbb{E}(y_{it}|H_{it})$ and $H_{it} = \{y_{i,t-1}, y_{i,t-2}, \dots\}$. Based on the data, model (3) can be rewritten into matrix form as follows:

$$\text{logit}(\mathbf{p}) = \mathbf{X}'\boldsymbol{\beta} + \mathbf{Z}, \quad \mathbf{Z} \sim \mathcal{N}(\mathbf{0}_N, \Sigma(\boldsymbol{\omega})), \quad (4)$$

where $\mathbf{p} = (\mathbf{p}_1', \dots, \mathbf{p}_T')'$, $\boldsymbol{\beta} = (\varphi_1, \dots, \varphi_R, \alpha_0, \boldsymbol{\alpha}', (\boldsymbol{\gamma}_1', \dots, \boldsymbol{\gamma}_L')')'$, $\boldsymbol{\omega} = (\sigma^2, \boldsymbol{\theta})'$, $\mathbf{Z} = (Z_1(\mathbf{x}_1), \dots, Z_1(\mathbf{x}_n), \dots, Z_T(\mathbf{x}_1), \dots, Z_T(\mathbf{x}_n))'$, \mathbf{X} is the model matrix $(X_1', \dots, X_T')'$, X_t is an $n \times (1 + R + d + dL)$ matrix with i -th row defined by $(X_t)_i = (1, y_{i,t-1}, \dots, y_{i,t-R}, \mathbf{x}_i', \mathbf{x}_i' y_{i,t-1}, \dots, \mathbf{x}_i' y_{i,t-L})$, and $\Sigma(\boldsymbol{\omega})$ is an $N \times N$ covariance matrix defined by

$$\Sigma(\boldsymbol{\omega}) = \sigma^2 \mathbf{R}_{\boldsymbol{\theta}} \otimes I_T \quad (5)$$

with $(\mathbf{R}_{\boldsymbol{\theta}})_{ij} = R_{\boldsymbol{\theta}}(\mathbf{x}_i, \mathbf{x}_j)$. Model (1) can also be rewritten in the same way by setting $R = 0, L = 0$ and $T = 1$.

With the presence of time series and their interaction with the input settings in model (3), we can write down the partial likelihood (PL) function (Cox, 1972, 1975) according to the formulation of Slud and Kedem (1994). Given the previous information $\{H_{it}\}_{i=1, \dots, n; t=1, \dots, N}$, the PL for $\boldsymbol{\beta}$ can be written as

$$PL(\boldsymbol{\beta}|\mathbf{Z}) = \prod_{i=1}^n \prod_{t=1}^T (p_{it}(\boldsymbol{\beta}|\mathbf{Z}))^{y_{it}} (1 - p_{it}(\boldsymbol{\beta}|\mathbf{Z}))^{1-y_{it}}, \quad (6)$$

where $p_{it}(\boldsymbol{\beta}|\mathbf{Z}) = \mathbb{E}_{\boldsymbol{\beta}|\mathbf{Z}}[y_{it}|H_{it}]$. Then, the integrated quasi-PL function for the estimation of $(\boldsymbol{\beta}, \boldsymbol{\omega})$ is given by

$$|\Sigma(\boldsymbol{\omega})|^{-1/2} \int \exp\{\log PL(\boldsymbol{\beta}|\mathbf{Z}) - \frac{1}{2}\mathbf{Z}'\Sigma(\boldsymbol{\omega})^{-1}\mathbf{Z}\}d\mathbf{Z}. \quad (7)$$

Note that, for model (1) where no time series effect is considered, (6) and (7) should be replaced by the likelihood function

$$L(\boldsymbol{\beta}|\mathbf{Z}) = \prod_{i=1}^n (p_{i1}(\boldsymbol{\beta}|\mathbf{Z}))^{y_{i1}} (1 - p_{i1}(\boldsymbol{\beta}|\mathbf{Z}))^{1-y_{i1}}$$

and the integrated quasi-likelihood function

$$|\Sigma(\boldsymbol{\omega})|^{-1/2} \int \exp\{\log L(\boldsymbol{\beta}|\mathbf{Z}) - \frac{1}{2}\mathbf{Z}'\Sigma(\boldsymbol{\omega})^{-1}\mathbf{Z}\}d\mathbf{Z} \quad (8)$$

respectively. Hereafter, we provide the framework for the integrated quasi-PL function (7), but the result can be applied to the integrated quasi-likelihood function (8) by assuming $R = 0, L = 0$ and $T = 1$.

Because of the difficulty in computing the integrated quasi-PL function, a *penalized quasi-PL* (PQPL) function is used as an approximation. Similar to the procedure in Breslow and Clayton (1993), the integrated quasi-partial log-likelihood can be approximated by Laplace's method (Barndorff-Nielsen and Cox, 1997). Ignoring the multiplicative constant and plugging (5) in $\Sigma(\boldsymbol{\omega})$, the approximation yields

$$\begin{aligned} & -\frac{1}{2} \log |I_n + \sigma^2 \mathbf{W}(\mathbf{R}_{\boldsymbol{\theta}} \otimes I_T)| + \\ & \sum_{i=1}^n \sum_{t=1}^T \left(y_{it} \log \frac{p_{it}(\boldsymbol{\beta}|\tilde{\mathbf{Z}})}{1 - p_{it}(\boldsymbol{\beta}|\tilde{\mathbf{Z}})} + \log(1 - p_{it}(\boldsymbol{\beta}|\tilde{\mathbf{Z}})) \right) - \frac{1}{2\sigma^2} \tilde{\mathbf{Z}}' (\mathbf{R}_{\boldsymbol{\theta}} \otimes I_T)^{-1} \tilde{\mathbf{Z}}, \end{aligned} \quad (9)$$

where \mathbf{W} is an $N \times N$ diagonal matrix with diagonal elements $W_{it} = p_{it}(\boldsymbol{\beta}|\tilde{\mathbf{Z}})(1 - p_{it}(\boldsymbol{\beta}|\tilde{\mathbf{Z}}))$, $p_{it}(\boldsymbol{\beta}|\tilde{\mathbf{Z}}) = \mathbb{E}_{\boldsymbol{\beta}|\tilde{\mathbf{Z}}}[y_{it}|H_{it}]$, and $\tilde{\mathbf{Z}} = \tilde{\mathbf{Z}}(\boldsymbol{\beta}, \boldsymbol{\omega})$ is the solution of $\sum_{i=1}^n \sum_{t=1}^T \mathbf{e}_{it}(y_{it} - p_{it}(\boldsymbol{\beta}|\mathbf{Z})) = (\mathbf{R}_{\boldsymbol{\theta}} \otimes I_T)^{-1} \mathbf{Z} / \sigma^2$, where \mathbf{e}_{it} is a unit-vector where $((t-1)n+i)$ -th element is one. The estimator $\hat{\boldsymbol{\beta}}$ which maximizes the PQPL function (9) is called *maximum quasi-PL estimator*. Thus, similar to the derivations in Breslow and Clayton (1993) for score equations of a penalized quasi-likelihood function, the score equations of the PQPL function for $\boldsymbol{\beta}$ and $\boldsymbol{\omega}$ are

$$\sum_{i=1}^n \sum_{t=1}^T X_{it}(y_{it} - p_{it}(\boldsymbol{\beta}, \boldsymbol{\omega})) = 0$$

and

$$\sum_{i=1}^n \sum_{t=1}^T \mathbf{e}_{it}(y_{it} - p_{it}(\boldsymbol{\beta}, \boldsymbol{\omega})) = (\mathbf{R}_{\boldsymbol{\theta}} \otimes I_T)^{-1} \mathbf{Z} / \sigma^2,$$

where $p_{it}(\boldsymbol{\beta}, \boldsymbol{\omega}) = \mathbb{E}_{\boldsymbol{\beta}, \boldsymbol{\omega}}[y_{it}|H_{it}]$. The solution to the score equations can be efficiently obtained by an iterated weighted least squares (IWLS) approach as follows. In each step, one first solves for $\boldsymbol{\beta}$ in

$$(\mathbf{X}' \mathbf{V}(\boldsymbol{\omega})^{-1} \mathbf{X}) \boldsymbol{\beta} = \mathbf{X}' \mathbf{V}(\boldsymbol{\omega})^{-1} \tilde{\boldsymbol{\eta}}, \quad (10)$$

where $\mathbf{V}(\boldsymbol{\omega}) = \mathbf{W}^{-1} + \sigma^2(\mathbf{R}_{\boldsymbol{\theta}} \otimes I_T)$, \mathbf{W} is an $N \times N$ diagonal matrix with diagonal elements $W_{it} = p_{it}(\boldsymbol{\beta}, \boldsymbol{\omega})(1 - p_{it}(\boldsymbol{\beta}, \boldsymbol{\omega}))$, and $\tilde{\eta}_{it} = \log \frac{p_{it}(\boldsymbol{\beta}, \boldsymbol{\omega})}{1 - p_{it}(\boldsymbol{\beta}, \boldsymbol{\omega})} + \frac{y_{it} - p_{it}(\boldsymbol{\beta}, \boldsymbol{\omega})}{p_{it}(\boldsymbol{\beta}, \boldsymbol{\omega})(1 - p_{it}(\boldsymbol{\beta}, \boldsymbol{\omega}))}$, and then sets

$$\hat{\mathbf{Z}} = \sigma^2(\mathbf{R}_{\boldsymbol{\theta}} \otimes I_T) \mathbf{V}(\boldsymbol{\omega})^{-1} (\tilde{\boldsymbol{\eta}} - \mathbf{X}' \hat{\boldsymbol{\beta}}) \quad (11)$$

and replaces $p_{it}(\boldsymbol{\beta}, \boldsymbol{\omega})$ with $p_{it}(\hat{\boldsymbol{\beta}}, \boldsymbol{\omega}) = \left(\frac{\exp\{\mathbf{X}' \hat{\boldsymbol{\beta}} + \hat{\mathbf{Z}}\}}{1 + \exp\{\mathbf{X}' \hat{\boldsymbol{\beta}} + \hat{\mathbf{Z}}\}} \right)_{it}$.

Estimation of the correlation parameters $\boldsymbol{\theta}$ and variance σ^2 is obtained by the restricted maximum likelihood (REML) approach (Patterson and Thompson, 1971) because it is known to have smaller bias comparing with the maximum likelihood approach (Patterson

and Thompson, 1974). According to Harville (1974, 1977), the REML estimators of σ^2 and $\boldsymbol{\theta}$ can be solved by minimizing the following negative log-likelihood function with respect to $\boldsymbol{\omega}$,

$$L(\boldsymbol{\omega}) = \frac{N-m}{2} \log(2\pi) - \frac{1}{2} \log(|\mathbf{X}'\mathbf{X}|) + \frac{1}{2} \log(|\mathbf{V}(\boldsymbol{\omega})|) + \frac{1}{2} \log(|\mathbf{X}'\mathbf{V}(\boldsymbol{\omega})^{-1}\mathbf{X}|) + \frac{1}{2} \tilde{\boldsymbol{\eta}}' \Pi(\boldsymbol{\omega}) \tilde{\boldsymbol{\eta}}, \quad (12)$$

where $m = 1 + R + d + dL$ and $\Pi(\boldsymbol{\omega}) = \mathbf{V}(\boldsymbol{\omega})^{-1} - \mathbf{V}(\boldsymbol{\omega})^{-1}\mathbf{X}(\mathbf{X}'\mathbf{V}(\boldsymbol{\omega})^{-1}\mathbf{X})^{-1}\mathbf{X}'\mathbf{V}(\boldsymbol{\omega})^{-1}$.

Therefore, the estimators $\hat{\boldsymbol{\beta}}$ and $\hat{\boldsymbol{\omega}}$ ($\equiv (\hat{\sigma}^2, \hat{\boldsymbol{\theta}})'$) can be obtained by iteratively solving (10), (11) and minimizing (12). The explicit algorithm is given in Appendix A. Note that $\mathbf{V}(\boldsymbol{\omega})$ is a block diagonal matrix, i.e., a square matrix having main diagonal blocks square matrices such that the off-diagonal blocks are zero matrices. Therefore the computational burden for the matrix inversion of $\mathbf{V}(\boldsymbol{\omega})$ can be alleviated by the fact that the inverse of a block diagonal matrix is a block diagonal matrix, composed of the inversion of each block.

3.2 Asymptotic Properties

Asymptotic results are presented here to show that the estimators $\hat{\boldsymbol{\beta}}$, $\hat{\sigma}^2$ and $\hat{\boldsymbol{\theta}}$ obtained in Section 3.1 are asymptotically normally distributed when $N (= nT)$ becomes sufficiently large. In the present context both n and T are sufficiently large. The assumptions are given in Appendix B, and the proofs are stated in Appendix C and D. These results are developed along the lines described in Hung et al. (2008) and Cressie and Lahiri (1993, 1996).

Theorem 3.1. *Under assumptions A1 and A2, the maximum quasi-PL estimator for the fixed effects $\boldsymbol{\beta}$ are consistent and asymptotically normal as $N \rightarrow \infty$,*

$$\sqrt{N}(\hat{\boldsymbol{\beta}} - \boldsymbol{\beta}) = \Lambda_N^{-1} \frac{1}{\sqrt{N}} S_N(\boldsymbol{\beta}, \boldsymbol{\omega}) + o_p(1)$$

and

$$\sqrt{N} \Lambda_N^{1/2} (\hat{\boldsymbol{\beta}} - \boldsymbol{\beta}) \xrightarrow{d} \mathcal{N}(\mathbf{0}, I_m),$$

where m is the size of the vector $\boldsymbol{\beta}$ (i.e., $m = 1 + R + d + dL$), the sample information matrix

$$\Lambda_N = \frac{1}{N} \sum_{i=1}^n \sum_{t=1}^T X_{it} X'_{it} p_{it}(\boldsymbol{\beta}, \boldsymbol{\omega}) (1 - p_{it}(\boldsymbol{\beta}, \boldsymbol{\omega})),$$

and $S_N(\boldsymbol{\beta}, \boldsymbol{\omega}) = \sum_{i=1}^n \sum_{t=1}^T X_{it} (y_{it} - p_{it}(\boldsymbol{\beta}, \boldsymbol{\omega})).$

Remark 3.2. For model (1), the estimator $\hat{\boldsymbol{\beta}}$ can be obtained by minimizing the penalized quasi-likelihood (PQL) function, which can be written as (9) with $T = 1$. Under assumption A1 and the application of central limit theorem, such estimator has the same asymptotic properties as in Theorem 3.1 with $N = n$.

For models (1) and (3), we have the following asymptotic properties for $\hat{\boldsymbol{\omega}}$.

Theorem 3.3. Denote $[\Gamma_N(\boldsymbol{\omega})]_{i,j} = \partial^2 L(\boldsymbol{\omega}) / \partial \omega_i \partial \omega_j$ and $J_N(\boldsymbol{\omega}) = [\mathbb{E}_{\boldsymbol{\omega}} \Gamma_N(\boldsymbol{\omega})]^{1/2}$. Then, under assumptions A3 and A4, as $N \rightarrow \infty$,

$$J_N(\hat{\boldsymbol{\omega}})(\hat{\boldsymbol{\omega}} - \boldsymbol{\omega}) \xrightarrow{d} \mathcal{N}(\mathbf{0}, I_{d+1}).$$

4 Construction of Predictive Distribution

For computer experiments, the construction of an optimal predictor and its corresponding predictive distribution is important for uncertainty quantification, sensitivity analysis, process optimization, and calibration (Santner et al., 2003).

First, some notation is introduced. For some untried setting \mathbf{x}_{n+1} , denote the predictive probability at time s by $p_s(\mathbf{x}_{n+1}) = \mathbb{E}[y_s(\mathbf{x}_{n+1})]$. Assume that $D_{n+1,s}$ represents the

“previous information” including $\{y_{it}, p_{it}\}$ and $\{y_{n+1,s-1}, y_{n+1,s-2}, \dots, p_{n+1,s-1}, p_{n+1,s-2}, \dots\}$ at \mathbf{x}_{n+1} , where $i = 1, \dots, n$ and $t = 1, \dots, T$. Also, let $\text{Logitnormal}(\mu, \sigma^2)$ represent a logit-normal distribution P , where $P = \exp\{X\}/(1 + \exp\{X\})$ and X has a univariate normal distribution with μ and variance σ^2 . Denote the first two moments of the distribution by $\mathbb{E}[P] = \kappa(\mu, \sigma^2)$ and $\mathbb{V}[P] = \tau(\mu, \sigma^2)$. In general, there is no closed form expression for $\kappa(\mu, \sigma^2)$ and $\tau(\mu, \sigma^2)$, but it can be easily computed by numerical integration such as in the package `logitnorm` (Wutzler, 2012) in `R` (R Core Team, 2015). More discussions on *logit-normal distribution* can be found in Mead (1965); Atchison and Shen (1980); Frederic and Lad (2008).

We first present a lemma which shows that, given $D_{n+1,s}$, the conditional distribution of $p_s(\mathbf{x}_{n+1})$ in model (3) is logit-normal. This result lays the foundation for the construction of predictive distribution. The proof is given in Appendix E.

Lemma 4.1. *For model (3), the conditional distribution of $p_s(\mathbf{x}_{n+1})$ can be written as*

$$p_s(\mathbf{x}_{n+1})|D_{n+1,s} \sim \text{Logitnormal}(m(D_{n+1,s}), v(D_{n+1,s})),$$

where

$$\begin{aligned} m(D_{n+1,s}) &= \sum_{r=1}^R \varphi_r y_{n+1,s-r} + \alpha_0 + \mathbf{x}'_{n+1} \boldsymbol{\alpha} + \sum_{l=1}^L \boldsymbol{\gamma}_l \mathbf{x}_{n+1} y_{n+1,s-l} + \mathbf{r}'_{\boldsymbol{\theta}} \mathbf{R}_{\boldsymbol{\theta}}^{-1} \left(\log \frac{\mathbf{p}_s}{\mathbf{1}_n - \mathbf{p}_s} - \boldsymbol{\mu}_s \right), \\ v(D_{n+1,s}) &= \sigma^2 (1 - \mathbf{r}'_{\boldsymbol{\theta}} \mathbf{R}_{\boldsymbol{\theta}}^{-1} \mathbf{r}_{\boldsymbol{\theta}}), \quad \mathbf{r}_{\boldsymbol{\theta}} = (R_{\boldsymbol{\theta}}(\mathbf{x}_{n+1}, \mathbf{x}_1), \dots, R_{\boldsymbol{\theta}}(\mathbf{x}_{n+1}, \mathbf{x}_n))', \quad \mathbf{R}_{\boldsymbol{\theta}} = \{R_{\boldsymbol{\theta}}(\mathbf{x}_i, \mathbf{x}_j)\}, \\ \mathbf{p}_s &= (p_s(\mathbf{x}_1), \dots, p_s(\mathbf{x}_n))', \text{ and } (\boldsymbol{\mu}_s)_i = \sum_{r=1}^R \varphi_r y_{i,s-r} + \alpha_0 + \mathbf{x}'_i \boldsymbol{\alpha} + \sum_{l=1}^L \boldsymbol{\gamma}_l \mathbf{x}_i y_{i,s-l}. \end{aligned}$$

Remark 4.2. For model (1), the result in Lemma 4.1 can be applied by having $R = 0, L = 0, s = 1$ and $T = 1$. Then, $D_{n+1,s}$ can be written as D_{n+1} containing only $\{p_{1,1}, \dots, p_{n,1}\}$,

and we have the conditional distribution

$$p(\mathbf{x}_{n+1})|D_{n+1} \sim \text{Logitnormal}(m(D_{n+1}), v(D_{n+1})),$$

where $m(D_{n+1}) = \mathbf{x}'_{n+1}\boldsymbol{\alpha} + \mathbf{r}'_{\boldsymbol{\theta}}\mathbf{R}_{\boldsymbol{\theta}}^{-1}(\log \frac{p_1}{1-p_1} - \boldsymbol{\mu}^n)$, $v(D_{n+1}) = \sigma^2(1 - \mathbf{r}'_{\boldsymbol{\theta}}\mathbf{R}_{\boldsymbol{\theta}}^{-1}\mathbf{r}_{\boldsymbol{\theta}})$, $\boldsymbol{\mu}^n = (\mathbf{x}'_1\boldsymbol{\alpha}, \dots, \mathbf{x}'_n\boldsymbol{\alpha})'$, $\mathbf{r}_{\boldsymbol{\theta}} = (R_{\boldsymbol{\theta}}(\mathbf{x}_{n+1}, \mathbf{x}_1), \dots, R_{\boldsymbol{\theta}}(\mathbf{x}_{n+1}, \mathbf{x}_n))'$, and $\mathbf{R}_{\boldsymbol{\theta}} = \{R_{\boldsymbol{\theta}}(\mathbf{x}_i, \mathbf{x}_j)\}$.

Based on Lemma 4.1, the prediction of $p_s(\mathbf{x}_{n+1})$ for some untried setting \mathbf{x}_{n+1} and its variance can then be obtained in the next theorem. The proof is given in Appendix F.

Theorem 4.3. *Given $D_{n+1,s} = \{\mathbf{y}'_1, \dots, \mathbf{y}'_T, \mathbf{p}'_1, \dots, \mathbf{p}'_T, y_{n+1,s-1}, \dots, y_{n+1,1}, p_{n+1,s-1}, \dots, p_{n+1,1}\}$,*

(i) the minimum mean squared error (MMSE) predictor of $p_s(\mathbf{x}_{n+1})$ is

$$\begin{aligned} \mathbb{E}[p_s(\mathbf{x}_{n+1})|D_{n+1,s}] &= \kappa(m(D_{n+1,s}), v(D_{n+1,s})) \\ \text{with variance } \mathbb{V}[p_s(\mathbf{x}_{n+1})|D_{n+1,s}] &= \tau(m(D_{n+1,s}), v(D_{n+1,s})); \end{aligned}$$

(ii) the MMSE predictor is an interpolator, i.e., if $\mathbf{x}_{n+1} = \mathbf{x}_i$ for $i = 1, \dots, n$, then

$$\mathbb{E}[p_s(\mathbf{x}_{n+1})|D_{n+1,s}] = p_s(\mathbf{x}_i) \text{ and } \mathbb{V}[p_s(\mathbf{x}_{n+1})|D_{n+1,s}] = 0;$$

(iii) the q -th quantile of the conditional distribution $p(\mathbf{x}_{n+1})|D_{n+1,s}$ is

$$\frac{\exp\{m(D_{n+1,s}) + z_q \sqrt{v(D_{n+1,s})}\}}{1 + \exp\{m(D_{n+1,s}) + z_q \sqrt{v(D_{n+1,s})}\}},$$

where z_q is the q -th quantile of the standard normal distribution.

Theorem 4.3 shows that, given $D_{n+1,s}$, the new predictor for binary data can interpolate the underlying probabilities which generate the training data. According to Theorem 4.3(iii) and the fact that $v(D_{n+1,s})$ increases with the distance to the training data, this result

shows an increasing predictive uncertainty for points away from the training data. This predictive property is desirable and consistent with the conventional GP predictor.

In practice, only the binary outputs are observable and the underlying probabilities are not available in the training data. Thus, the following results construct the MMSE predictor of $p_s(\mathbf{x}_{n+1})$ given $\mathbf{Y} = (\mathbf{y}'_1, \dots, \mathbf{y}'_T, y_1(\mathbf{x}_{n+1}), \dots, y_{s-1}(\mathbf{x}_{n+1}))'$. These results can be used for prediction and quantification of the predictive uncertainty, such as constructing predictive confidence intervals for untried settings.

Corollary 4.4. *Given $\mathbf{Y} = (\mathbf{y}'_1, \dots, \mathbf{y}'_T, y_1(\mathbf{x}_{n+1}), \dots, y_{s-1}(\mathbf{x}_{n+1}))'$,*

(i) The MMSE predictor of $p_s(\mathbf{x}_{n+1})$ is

$$\mathbb{E} [p_s(\mathbf{x}_{n+1})|\mathbf{Y}] = \mathbb{E}_{\mathbf{p}|\mathbf{Y}} [\kappa(m(D_{n+1,s}), v(D_{n+1,s}))|\mathbf{Y}] \quad (13)$$

with variance

$$\mathbb{V} [p_s(\mathbf{x}_{n+1})|\mathbf{Y}] = \mathbb{E}_{\mathbf{p}|\mathbf{Y}} [\tau(m(D_{n+1,s}), v(D_{n+1,s}))|\mathbf{Y}] + \mathbb{V}_{\mathbf{p}|\mathbf{Y}} [\kappa(m(D_{n+1,s}), v(D_{n+1,s}))|\mathbf{Y}], \quad (14)$$

where $\mathbf{p} = (\mathbf{p}'_1, \dots, \mathbf{p}'_T, p_1(\mathbf{x}_{n+1}), \dots, p_{s-1}(\mathbf{x}_{n+1}))'$.

(ii) When $\mathbf{x}_{n+1} = \mathbf{x}_i$, the MMSE predictor becomes $\mathbb{E}_{\mathbf{p}|\mathbf{Y}} [p_s(\mathbf{x}_i)|\mathbf{Y}]$ and the variance becomes $\mathbb{V}_{\mathbf{p}|\mathbf{Y}} [p_s(\mathbf{x}_i)|\mathbf{Y}]$.

Remark 4.5. For model (1), the results of Theorem 4.3 and Corollary 4.4 can be applied by assuming $s = 1$ and $T = 1$.

Without the information of the underlying probabilities, the predictor does not interpolate all the training data as in Theorem 4.3 (ii). From Corollary 4.4, when $\mathbf{x}_{n+1} = \mathbf{x}_i$, the predictor is still unbiased but the corresponding variance is nonzero. Instead, the variance

becomes $\mathbb{V}_{\mathbf{p}|\mathbf{Y}} [p_s(\mathbf{x}_i)|\mathbf{Y}]$, which is due to the uncertainty of the underlying probability. The proof is similar to Theorem 4.3 (ii). To show the empirical performance of the predictive distribution in Corollary 4.4, a one-dimensional example is illustrated in Figure 1. Consider the true probability function, $p(x) = 0.4 \exp(-1.2x) \cos(3.5\pi x) + 0.4$, which is represented by a black dotted line, and the training set that contains 12 evenly-spaced inputs and the corresponding binary outputs represented by red dots. The blue line is the MMSE predictor constructed by equation (13) and the gray region is the corresponding 95% confidence band constructed by the 2.5%- and 97.5%-quantiles. It appears that the proposed predictor and the confidence band reasonably capture the underlying probability.

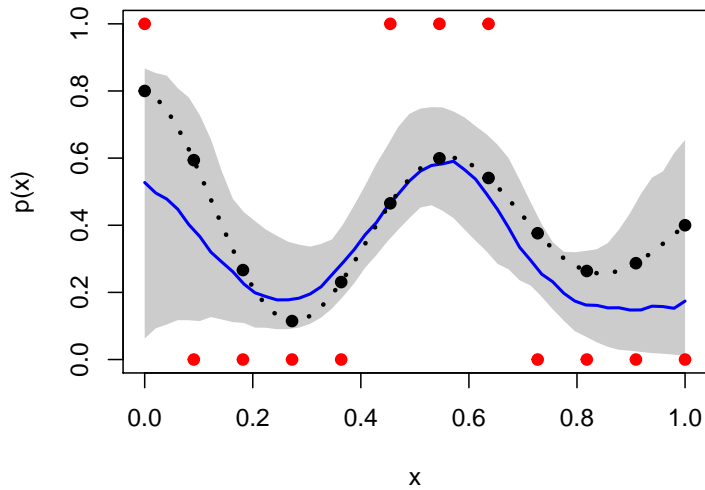


Figure 1: Illustration of predictive distribution. Black dotted line represents the true probability function, red dots represent the binary response data, black dots represent the true probabilities at the chosen locations, and the emulator is represented by the blue line, with the gray shaded region providing a pointwise 95% confidence band.

Although there is no closed form expression for the distribution of $\mathbf{p}|\mathbf{Y}$, the random samples from $\mathbf{p}|\mathbf{Y}$ can be easily generated by the Metropolis-Hastings (MH) algorithm. See Appendix G for the explicit algorithm. Based on these samples, the expectation and

variance in Corollary 4.4 can be approximated by using a Monte Carlo method. For example, let $\{\mathbf{p}^{(j)}\}_{j=1,\dots,J}$ be the J random samples generated from distribution $\mathbf{p}|\mathbf{Y}$, then the MMSE predictor of $p_s(\mathbf{x}_{n+1})$ in Corollary 4.4 can be approximated by

$$\mathbb{E}_{\mathbf{p}|\mathbf{Y}} [\kappa(m(D_{n+1,s}), v(D_{n+1,s}))|\mathbf{Y}] \approx \frac{1}{J} \sum_{j=1}^J \kappa(m(D_{n+1,s}^{(j)}), v(D_{n+1,s}^{(j)})),$$

where $D_{n+1,s}^{(j)} = \{\mathbf{p}^{(j)}, \mathbf{Y}\}$. Similar idea can be applied to compute $\mathbb{V}[p_s(\mathbf{x}_{n+1})|\mathbf{Y}]$. The quantiles of $p_s(\mathbf{x}_{n+1})|\mathbf{Y}$ can be obtained from a sample $\{p_s^{(1)}, \dots, p_s^{(J)}\}$, where $p_s^{(j)}$ is generated from $p_s(\mathbf{x}_{n+1})|D_{n+1,s}^{(j)}$ following a logit-normal distribution by Lemma 4.1.

When the historical time series for an untried setting (i.e., $y_1(\mathbf{x}_{n+1}), \dots, y_{s-1}(\mathbf{x}_{n+1})$ in Corollary 4.4) is not available, we can emulate a completely new time series (or batch of time series) with input \mathbf{x}_{n+1} . The idea is to generate draws from the conditional distribution $p_s(\mathbf{x}_{n+1})|\mathbf{Y}$ for future outputs, starting from $s = 0$, and take pointwise median of the random draws. This idea is similar to the dynamic emulators introduced by Liu and West (2009) for continuous outputs. The random samples from $p_s(\mathbf{x}_{n+1})|\mathbf{Y}$ can be generated by the fact $f(p_s(\mathbf{x}_{n+1}), \mathbf{p}|\mathbf{Y}) = f(\mathbf{p}|\mathbf{Y})f(p_s(\mathbf{x}_{n+1})|\mathbf{p}, \mathbf{Y})$, where $f(p_s(\mathbf{x}_{n+1})|\mathbf{p}, \mathbf{Y})$ is a logit-normal distribution provided in Lemma 4.1. As mentioned above, the random samples from $f(\mathbf{p}|\mathbf{Y})$ can be generated through the MH algorithm. Therefore, generating a draw from $p_s(\mathbf{x}_{n+1})|\mathbf{Y}$ consists of two steps: (1) generating the “previous” probability values \mathbf{p}^* given output \mathbf{Y} from the distribution $\mathbf{p}|\mathbf{Y}$ through the MH algorithm, and (2) based on the sample \mathbf{p}^* , draw a sample $p_s^*(\mathbf{x}_{n+1})$ from $p_s(\mathbf{x}_{n+1})|\mathbf{p}^*, \mathbf{Y}$, which is a logit-normal distribution, and also draw a sample $y_s^*(\mathbf{x}_{n+1})$ from a Bernoulli distribution with parameter $p_s^*(\mathbf{x}_{n+1})$. An explicit algorithm is given in Appendix H.

5 Simulation Studies

In Section 5.1, we conduct simulations generated from Gaussian processes to demonstrate the estimation performance. In Section 5.2, the prediction performance is examined by comparing several existing methods using the data generated from a modified Friedman function (Friedman, 1991).

5.1 Estimation Performance

Consider a 5-dimensional input space, $d = 5$, and the input \mathbf{x} is randomly generated from a regular grid on $[0, 1]^5$. The binary output, $y_t(\mathbf{x})$ at time t , is simulated by a Bernoulli distribution with probability $p_t(\mathbf{x})$ calculated by (3) and $\alpha_0 = 0.5$, $\boldsymbol{\alpha} = (-3, 2, -2, 1, 0.5)'$, $\varphi_1 = 0.8$, $\sigma^2 = 1$, and the power exponential correlation function (2) is chosen with $\boldsymbol{\theta} = (0.5, 1.0, 1.5, 2.0, 2.5)'$ and $p = 2$. Four sample size combinations of n and T are considered in the simulations.

Apart from the power exponential correlation function (abbreviated as PE), we also consider the orthogonal correlation function (abbreviated as OGP) proposed by Plumlee and Joseph (2018), which addresses the identifiability issues in conventional GP modeling. The orthogonal correlation function is derived from the power exponential correlation function. Details can be found in Section 3 of Plumlee and Joseph (2018).

The estimation results for the linear function coefficients are summarized in Table 1 based on 100 replicates for each sample size combination. In general, the proposed approach can estimate the linear function coefficients $(\alpha_0, \boldsymbol{\alpha}, \varphi_1)$ reasonably well. Comparing with PE, it appears that the estimation accuracy is further improved by the use of orthogonal correlation functions. Therefore, *orthogonal correlation functions are generally recommended* if estimation is of major interest, such as in variable selection and calibration problems.

n	T	Corr	$\hat{\alpha}_0$	$\hat{\alpha}_1$	$\hat{\alpha}_2$	$\hat{\alpha}_3$	$\hat{\alpha}_4$	$\hat{\alpha}_5$	$\hat{\varphi}_1$
200	20	PE	0.46 (0.11)	-2.71 (0.15)	1.82 (0.13)	-1.82 (0.12)	0.91 (0.09)	0.46 (0.10)	0.72 (0.11)
		OGP	0.48 (0.12)	-2.77 (0.12)	1.84 (0.10)	-1.85 (0.09)	0.91 (0.08)	0.46 (0.08)	0.71 (0.10)
	50	PE	0.45 (0.07)	-2.68 (0.10)	1.80 (0.09)	-1.79 (0.08)	0.90 (0.07)	0.46 (0.06)	0.70 (0.07)
		OGP	0.47 (0.08)	-2.75 (0.09)	1.83 (0.06)	-1.83 (0.06)	0.92 (0.06)	0.46 (0.05)	0.71 (0.08)
500	20	PE	0.47 (0.09)	-2.76 (0.14)	1.82 (0.12)	-1.83 (0.10)	0.91 (0.08)	0.48 (0.07)	0.73 (0.07)
		OGP	0.49 (0.08)	-2.81 (0.09)	1.89 (0.07)	-1.88 (0.06)	0.95 (0.06)	0.46 (0.06)	0.74 (0.07)
	50	PE	0.45 (0.06)	-2.75 (0.07)	1.83 (0.06)	-1.83 (0.06)	0.92 (0.06)	0.45 (0.05)	0.74 (0.04)
		OGP	0.47 (0.06)	-2.80 (0.05)	1.87 (0.04)	-1.87 (0.04)	0.93 (0.03)	0.47 (0.03)	0.75 (0.04)

Table 1: Estimation of linear coefficients. The values are the average estimates over 100 replicates, while the values in parentheses are the standard deviation of the estimates. The parameter settings are $\alpha_0 = 0.5$, $\alpha_1 = -3$, $\alpha_2 = 2$, $\alpha_3 = -2$, $\alpha_4 = 1$, $\alpha_5 = 0.5$, and $\varphi_1 = 0.8$.

The parameter estimation results for σ^2 and PE correlation parameters $\boldsymbol{\theta}$ is reported in Table 2. The estimation with OGP has similar results, so we omit them to save space. The proposed approach tends to overestimate the correlation parameters for small sample size. This is not surprising because the estimation of correlation parameters is more challenging and the same phenomenon is observed in conventional GP models (see Li and Sudjianto (2005)). This problem can be ameliorated by the increase of sample size as shown in Table 2. Given the same number of total sample size, $(n = 200, T = 50)$ and $(n = 500, T = 20)$, it appears that a larger n can improve the estimation accuracy more effectively.

n	T	$\hat{\theta}_1$	$\hat{\theta}_2$	$\hat{\theta}_3$	$\hat{\theta}_4$	$\hat{\theta}_5$	$\hat{\sigma}^2$
200	20	0.86 (0.81)	1.80 (1.13)	2.35 (1.41)	3.30 (1.76)	4.10 (1.85)	0.82 (0.07)
200	50	0.65 (0.16)	1.55 (0.63)	2.38 (1.12)	3.01 (1.25)	3.80 (1.49)	0.79 (0.05)
500	20	0.61 (0.16)	1.17 (0.25)	1.93 (0.54)	2.66 (0.96)	3.24 (1.17)	0.87 (0.05)
500	50	0.57 (0.08)	1.16 (0.16)	1.78 (0.35)	2.37 (0.39)	3.11 (0.68)	0.87 (0.03)

Table 2: Estimation of correlation parameters and variance. The values are the average estimates over 100 replicates, while the values in parentheses are the standard deviation of the estimates. The parameter settings are $\theta_1 = 0.5$, $\theta_2 = 1.0$, $\theta_3 = 1.5$, $\theta_4 = 2$, $\theta_5 = 2.5$, and $\sigma^2 = 1$.

Based on the construction of predictive distribution in Section 4, we can emulate a new time series with an untried input. Here we generate 100 random untried inputs to examine its prediction performance. The prediction performance is evaluated by the following two measures. Define the 100 random untried inputs ($n_{\text{test}} = 100$) as $\mathbf{x}_1^*, \dots, \mathbf{x}_{100}^*$, the root mean squared prediction error is calculated by

$$\text{RMSPE} = \left(\frac{1}{n_{\text{test}} T} \sum_{i=1}^{n_{\text{test}}} \sum_{t=1}^T (p_t(\mathbf{x}_i^*) - \hat{p}_t(\mathbf{x}_i^*))^2 \right)^{1/2}$$

and its misclassification rate (MR) is calculated by

$$\frac{1}{n_{\text{test}} T} \sum_{i=1}^{n_{\text{test}}} \sum_{t=1}^T (y_t(\mathbf{x}_i^*) - \hat{y}_t(\mathbf{x}_i^*))^2,$$

where $\hat{p}_t(\mathbf{x}_i^*)$ and $\hat{y}_t(\mathbf{x}_i^*)$ are respectively the predictive probability and the predictive binary response by the proposed method. The RMSPE and MR results are given in Table 3.

Overall, the proposed predictor has the root mean squared prediction error less than 0.12 and the misclassification rate less than 17.3%. Also, with the increase of sample size, the prediction error, in terms of both RMSPE and MR, decreases in general.

	$n = 200$ $T = 20$	$n = 200$ $T = 50$	$n = 500$ $T = 20$	$n = 500$ $T = 50$
RMSPE	0.1188 (0.0066)	0.1193 (0.0058)	0.1058 (0.0060)	0.1053 (0.0045)
MR (%)	17.22 (1.55)	17.27 (1.39)	17.08 (1.58)	16.83 (1.19)

Table 3: Comparison of RMSPEs and misclassification rates.

Furthermore, the predictive distributions can be used to quantify the prediction uncertainty. The predictive distributions with two random untried inputs are shown in Figure 2, where the green dotted lines represent the true probability, the red dashed lines represent the MMSE predictors obtained in Corollary 4.4. From Figure 2, it appears that the MMSE predictors provide accurate predictions in both cases. Moreover, the predictive distributions provide rich information for statistical inference. For example, we can construct 95% predictive confidence intervals for the two untried settings as indicated in blue in Figure 2.

5.2 Prediction Performance

To examine the performance of the proposed model as an emulator, we compare its prediction accuracy with four existing methods: (1) the logistic regression model, (2) a combination of logistic regression model with time series mean function, (3) the Bayesian generalized Gaussian process model (Williams and Barber, 1998), which incorporates a Gaussian process prior but does not take into account the time series structure, and (4) the functional

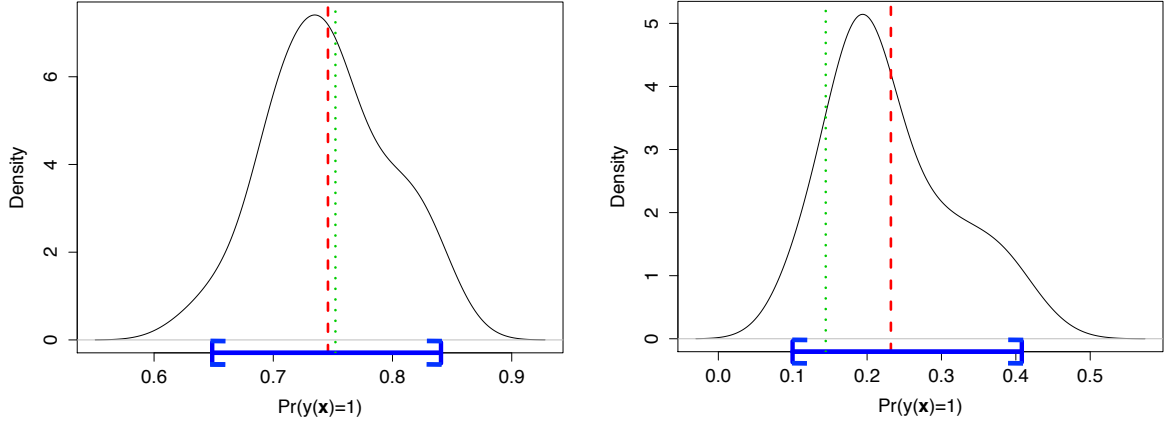


Figure 2: Predictive distributions. The green dotted lines are the true probability, the red dashed lines are the MMSE predictors, and the 95% predictive confidence intervals are indicated in blue.

Gaussian process proposed by Shi and Choi (2011), which captures the serial correlation by functional data analysis techniques. These methods are respectively implemented by R (R Core Team, 2015) using packages **binaryGP** (Sung, 2017), **stat** (R Core Team, 2015), a modification of **stat**, **kernlab** (Karatzoglou et al., 2004) and **GPFDA** (Shi and Cheng, 2014) adapted to classification.

The simulated data are generated by a modification of the Friedman function (Friedman, 1991),

$$\text{logit}(p_t(\mathbf{x})) = y_{t-1}(\mathbf{x}) + \frac{1}{3} [10 \sin(\pi x_1 x_2) + 20(x_3 - 0.5)^2 + 10x_4 + 5x_5] - 5,$$

where $\mathbf{x} \in [0, 1]^5$ and the Friedman function is given in the brackets with intercept -5 and scale $1/3$ to ensure $p_t(\mathbf{x})$ is uniformly located at $[0, 1]$. The input \mathbf{x} is randomly generated from $[0, 1]^5$ and the corresponding binary output $y_t(\mathbf{x})$ at time t is generated by a Bernoulli distribution with probability $p_t(\mathbf{x})$. The size of the training data is set to be $n = 200, T = 20$.

The prediction performance is evaluated by RMSPE using 100 randomly generated

untried settings ($n_{\text{test}} = 100, T = 20$). The results for the four methods based on 100 replicates are shown in Figure 3. In general, the proposed method has lower RMSPE than the other four methods. By incorporating a Gaussian process to model the nonlinearity, the proposed method outperforms the straightforward combination of logistic regression model and time series structure. On the other hand, comparing with Bayesian generalized Gaussian process model (i.e., kernlab in Figure 3), the proposed method further improves the prediction accuracy by taking into account the time series structure.

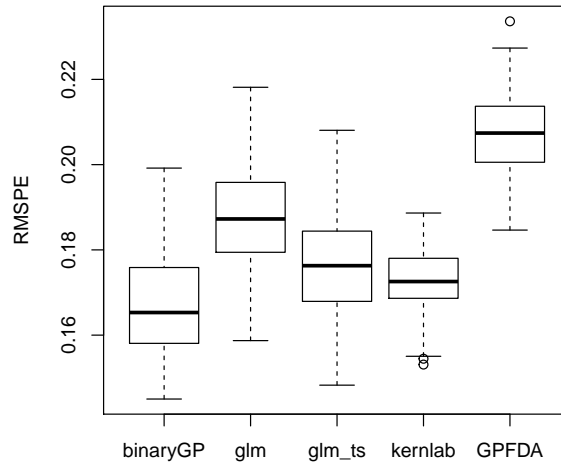


Figure 3: Comparison of prediction performance. *binaryGP*: proposed method, *glm*: logistic regression, *glm_ts*: logistic regression with time-series mean function, *kernlab*: Bayesian generalized GP, and *GPFDA*: functional Gaussian process model.

6 Computer Experiments for Cell Adhesion Frequency Assay

In an earlier study based on *in vitro* experiments, an important memory effect was discovered in the repeated adhesion experiments of the micropipette adhesion frequency assay. However, only limited variables of interest can be studied in the lab because of the technical complexity of the biological setting and the complicated experimental manipulation. Therefore, computer simulation experiments are performed to examine the complex mechanisms behind repeated receptor-ligand binding to rigorously elucidate the biological mechanisms behind the memory effect.

In these computer experiments, two surfaces are simulated to reflect the two opposing membranes in the adhesion frequency assays. The molecules on the surfaces are permitted to interact for the contact duration and then separated for a period of waiting time to simulate the retract-approach phase of the assays. The computer experiments are constructed based on a kinetic proofreading model for receptor modification or other induced mechanisms (to be described later) and solved through a Gillespie algorithm. The contact is scored as 1 or 0 depending on whether at least one bond or no bond is observed, respectively. The process is repeated until the given number of contacts is completed.

The biological system investigated here is the T Cell Receptor (TCR) binding to antigen peptide bound to Major Histocompatibility Complex (pMHC), which has previously been shown to exhibit memory in repeated contacts (Zarnitsyna et al., 2007). The TCR is the primary molecule involved in detecting foreign antigens which are presented on pMHC molecules expressed by infected cells. Memory in serial interactions of these foreign antigens may be a mechanism which underlies the major properties of T cell antigen recognition: sensitivity, specificity, and context discrimination. It has largely remained uninvestigated

due to the small time scales at which the mechanism operates and the complexity of the experimental system. Although there are many possible cellular mechanisms which may induce this behavior, two specific mechanisms are proposed and investigated in this study as to how this memory may be controlled: 1) pMHC binding to a single TCR within a cluster upregulates the kinetics of all TCRs within that cluster, or 2) pulling by engaged pMHC of a single TCR within a cluster induces upregulated kinetics to the cluster of TCRs. The two mechanisms are called free induction mechanism and forced induction mechanism for brevity. The difference between the two is that the free induction mechanism only considers bonds that are spontaneously dissociated during the contact period before retraction pulls the two cells apart, hence would not have experienced any force, whereas the forced-induction mechanism only considers bonds that are forced to dissociate during retraction, hence would have experienced pulling force (Huang et al., 2010).

The free induction mechanism has six control variables given in Table 4. The range of each control variable in Table 4 is given by physical principles or estimated through similar molecular interactions. The design of the control variables is a 60-run OA-based Latin hypercube designs (Tang, 1993). For each run, it consists of 50 replicates and each replicate has 100 repeated contacts ($T = 100$).

Variable	Description	Range
$x_{K_{f,p}}$	on-rate enhancement of activated TCRs	(1,100)
$x_{K_{r,p}}$	off-rate enhancement of activated TCRs	(0.1,100)
$x_{T_{half}}$	half-life of cluster activation	(0.1,10)
x_{T_c}	cell-cell contact time	(0.1,10)
x_{T_w}	waiting time in between contacts	(0.1,10)
x_{K_c}	kinetic proofreading modification rate for activation of cluster	(0.1,10)

Table 4: *Control variables in cell adhesion frequency assay experiments.*

The proposed estimation method is implemented with orthogonal correlation functions derived from the power exponential correlation function with $p = 2$. We start with a large model in which the mean function includes all the main effects of the control variables and their interactions with the past time series output y_{t-1} . The model is written as:

$$\text{logit}(p_t(\mathbf{x})) = -0.07 + \hat{\varphi}_1 y_{t-1}(\mathbf{x}) + \hat{\alpha}_1 x_{K_{f,p}} + \hat{\alpha}_2 x_{K_{r,p}} + \hat{\alpha}_3 x_{T_{half}} + \hat{\alpha}_4 x_{Tc} + \hat{\alpha}_5 x_{Tw} + \hat{\alpha}_6 x_{Kc} + (\hat{\gamma}_1 x_{K_{f,p}} + \hat{\gamma}_2 x_{K_{r,p}} + \hat{\gamma}_3 x_{T_{half}} + \hat{\gamma}_4 x_{Tc} + \hat{\gamma}_5 x_{Tw} + \hat{\gamma}_6 x_{Kc}) y_{t-1}(\mathbf{x}) + Z_t(\mathbf{x}),$$

where all the control variables are standardized to $[0, 1]$, $\hat{\sigma} = 0.43$ and the estimated correlation parameters are $\hat{\boldsymbol{\theta}} = (\hat{\theta}_{K_{f,p}}, \hat{\theta}_{K_{r,p}}, \hat{\theta}_{T_{half}}, \hat{\theta}_{Tc}, \hat{\theta}_{Tw}, \hat{\theta}_{Kc}) = (3.28, 1.70, 7.77, 0.06, 4.78, 0.74)$. Estimation results for the mean function coefficients are given in Table 5 with p values calculated based on the asymptotic results in Theorem 3.1. We use these p values to perform variable selection and identify significant effects for the mean function. According to Table 5, $x_{T_{half}}$ has no significant effect in the mean function at the 0.01 level. By removing $x_{T_{half}}$, the model can be updated as

$$\text{logit}(p_t(\mathbf{x})) = -0.07 + 0.14 y_{t-1}(\mathbf{x}) + 0.13 x_{K_{f,p}} + 0.37 x_{K_{r,p}} + 0.47 x_{Tc} - 0.08 x_{Tw} + 0.15 x_{Kc} + (0.16 x_{K_{f,p}} + 0.23 x_{K_{r,p}} - 0.09 x_{T_{half}} + 0.23 x_{Tc} - 0.17 x_{Tw} + 0.36 x_{Kc}) y_{t-1}(\mathbf{x}) + Z_t(\mathbf{x}),$$

where $\hat{\sigma} = 0.44$, the estimated correlation parameters are $\hat{\boldsymbol{\theta}} = (\hat{\theta}_{K_{f,p}}, \hat{\theta}_{K_{r,p}}, \hat{\theta}_{T_{half}}, \hat{\theta}_{Tc}, \hat{\theta}_{Tw}, \hat{\theta}_{Kc}) = (3.27, 1.71, 7.77, 0.06, 4.81, 0.74)$.

The forced induction mechanism has five control variables which are the same as the first five in the free induction mechanism (except that x_{Kc} is removed). Similar to the

	Standard			
	Value	deviation	Z score	p value
$\hat{\varphi}_1$	0.14	0.02	7.96	0.0000
$\hat{\alpha}_1$	0.13	0.02	5.96	0.0000
$\hat{\alpha}_2$	0.37	0.02	17.82	0.0000
$\hat{\alpha}_3$	0.00	0.02	0.08	0.9331
$\hat{\alpha}_4$	0.47	0.02	22.54	0.0000
$\hat{\alpha}_5$	-0.08	0.02	-3.79	0.0001
$\hat{\alpha}_6$	0.15	0.02	6.86	0.0000
$\hat{\gamma}_1$	0.16	0.03	5.2	0.0000
$\hat{\gamma}_2$	0.23	0.03	7.68	0.0000
$\hat{\gamma}_3$	-0.09	0.03	-2.92	0.0035
$\hat{\gamma}_4$	0.23	0.03	7.28	0.0000
$\hat{\gamma}_5$	-0.17	0.03	-5.47	0.0000
$\hat{\gamma}_6$	0.36	0.03	11.83	0.0000

Table 5: Estimation results for the free induction mechanism.

analysis procedure before, the following model can be obtained:

$$\text{logit}(p_t(\mathbf{x})) = -0.21 + \hat{\varphi}_1 y_{t-1}(\mathbf{x}) + \hat{\alpha}_1 x_{K_{f,p}} + \hat{\alpha}_2 x_{K_{r,p}} + \hat{\alpha}_3 x_{T_{half}} + \hat{\alpha}_4 x_{Tc} + \hat{\alpha}_5 x_{Tw} + (\hat{\gamma}_1 x_{K_{f,p}} + \hat{\gamma}_2 x_{K_{r,p}} + \hat{\gamma}_3 x_{T_{half}} + \hat{\gamma}_4 x_{Tc} + \hat{\gamma}_5 x_{Tw}) y_{t-1}(\mathbf{x}) + Z_t(\mathbf{x}),$$

where all the control variables are standardized to $[0, 1]$, $\hat{\sigma} = 0.38$, the estimated correlation parameters are $\hat{\boldsymbol{\theta}} = (\hat{\theta}_{K_{f,p}}, \hat{\theta}_{K_{r,p}}, \hat{\theta}_{T_{half}}, \hat{\theta}_{Tc}, \hat{\theta}_{Tw}) = (5.16, 1.02, 3.64, 0.12, 10.55)$, and the estimation and inference results for the mean function coefficients are given in Table 6. It can be seen from Table 6 that, with the same significant level, the forced induction mechanism is dominated by only four effects in the mean function, which is a smaller model compared to that for the free induction mechanism. By removing the insignificant effects,

the final model can be written as:

$$\text{logit}(p_t(\mathbf{x})) = -0.21 + 0.09y_{t-1} + 0.09x_{K_{f,p}} + 0.11x_{K_{r,p}} + 0.27x_{Tc} + Z_t(\mathbf{x}),$$

where $\hat{\sigma} = 0.38$ and the estimated correlation parameters are $\hat{\boldsymbol{\theta}} = (\hat{\theta}_{K_{f,p}}, \hat{\theta}_{K_{r,p}}, \hat{\theta}_{T_{half}}, \hat{\theta}_{Tc}, \hat{\theta}_{Tw}) = (6.81, 0.90, 3.50, 0.11, 10.88)$.

	Standard			
	Value	deviation	Z score	p value
$\hat{\varphi}_1$	0.10	0.02	5.24	0.0000
$\hat{\alpha}_1$	0.08	0.02	3.57	0.0004
$\hat{\alpha}_2$	0.08	0.02	3.76	0.0002
$\hat{\alpha}_3$	-0.03	0.02	-1.22	0.2222
$\hat{\alpha}_4$	0.28	0.02	13.69	0.0000
$\hat{\alpha}_5$	-0.01	0.02	-0.31	0.7549
$\hat{\gamma}_1$	-0.03	0.04	-0.76	0.4448
$\hat{\gamma}_2$	0.08	0.03	2.56	0.0103
$\hat{\gamma}_3$	-0.02	0.03	-0.49	0.6238
$\hat{\gamma}_4$	-0.04	0.03	-1.2	0.2311
$\hat{\gamma}_5$	0.06	0.03	1.84	0.0664

Table 6: *Estimation results for the forced induction mechanism.*

By comparing the analyses of the two mechanisms, we see several significant differences, which cannot be directly observed experimentally. The fitted models show that among the interaction effects, all the control variables except $x_{T_{half}}$ are significant for inducing memory in the free induction model, whereas no interaction effects are significant in the force induction model. The application of this statistical approach to the analysis of simulations and experimental data will be powerful in illuminating the unknown biological mechanism, and also informs the next round of experiments by advising future manipulations. Additionally, developments on the calibration of computer experiments based upon the

proposed predictive distribution will help provide insight into the range of possible values of variables, such as the increases in kinetic rates, which are difficult to determine through existing methods due to the small time scale at which this mechanism operates and the limits of existing experimental techniques.

Besides estimation, the proposed method also provides predictors which can serve as efficient and accurate emulators for untried computer experiments. The construction of emulator is an important step for future research on calibration where computer experiment outputs under the same settings of the lab experiments are required but not necessarily available. To assess the predictive performance, we compare the proposed predictor with the four existing methods discussed in Section 5 based on a 10-fold cross-validation study. The prediction errors for the two mechanisms are reported in Figure 4. For both mechanisms, the proposed predictor has a smaller prediction error compared with the other alternatives. It also appears that the new predictor provides more predictive improvement in the first mechanism, the free induction mechanism. A plausible explanation is that the underlying memory effects and the interaction effect between time series and control settings are higher in the free induction mechanism and they are properly captured in the proposed predictor.

7 Summary and Concluding Remarks

In spite of the prevalence of Gaussian process models in the analysis of computer experiments, their applications are limited to the Gaussian assumption on the responses. Motivated by the study of cell adhesion where the computer simulation responses are binary time series, a generalized Gaussian process model is proposed in this paper. The estimation procedure is introduced and asymptotic properties are derived. An optimal predictor and its predictive distribution are constructed which can be used for uncertainty quantification

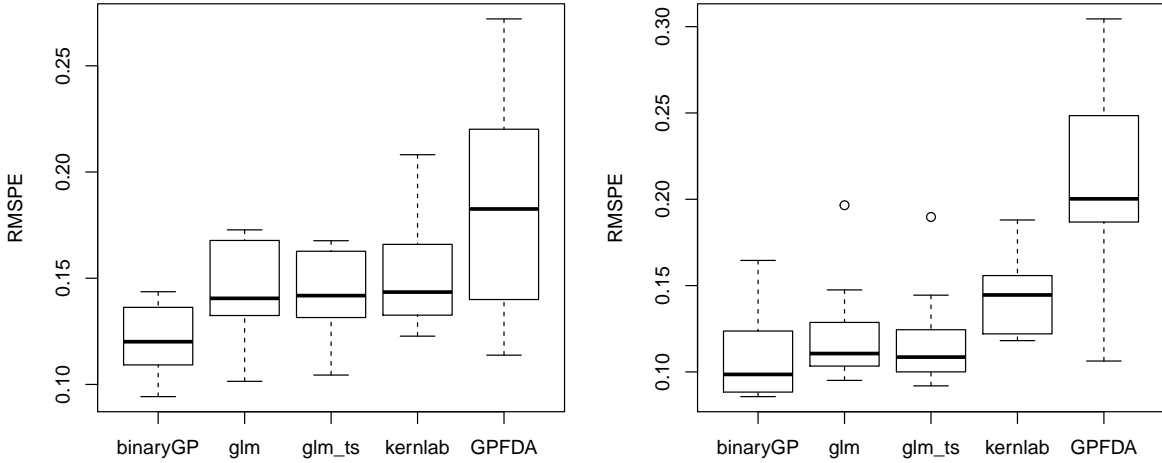


Figure 4: Comparison of prediction performance for the free induction mechanism (left panel) and for the forced induction mechanism (right panel). *binaryGP*: proposed method, *glm*: logistic regression, *glm_ts*: logistic regression with time-series mean function, *kernlab*: Bayesian generalized GP, and *GPFDA*: functional Gaussian process model.

and calibration of future computer simulations. An R package is available for implementing the proposed methodology. The methodology is applied to analyze computer simulations of two cell adhesion mechanisms. The results reveal significant differences between the two mechanisms and provide valuable insights on how the next round of lab experiments should be conducted.

The current work can be extended in several directions. First, we will extend the proposed method to other non-Gaussian data, such as the count data. It is conceivable that the current estimation procedure can be directly extended to other exponential family distributions, but different predictive distributions are expected for different types of non-Gaussian data. Second, the computational cost in the proposed procedure can be further reduced. In particular, the inversion of \mathbf{R}_θ can be computationally prohibitive when sample

size is large. This computational issue has been addressed for conventional GP models in the recent literature. Extensions of these methods (e.g., Gramacy and Apley (2015); Sung et al. (2018)) to binary responses deserve further attention. Third, many mathematical models underlying the computer simulations contain unknown parameters, which need to be estimated using data from lab experiments. This problem is called calibration and much work has been done in the computer experiment literature. However, the existing methods (e.g., Kennedy and O'Hagan (2001), Tuo and Wu (2015) and Gramacy et al. (2015)) are only applicable under the Gaussian assumption. Based upon the model and prediction procedure proposed herein, we will work on developing a calibration method for non-Gaussian data.

Acknowledgements: The authors gratefully acknowledge helpful advice from the associate editor and two referees. This work was supported by NSF DMS 1660504 and 1660477.

Appendices

A Algorithm: Estimation of (β, ω)

- 1: Set initial values $\omega = (\sigma^2, \theta) = \mathbf{1}_{d+1}, \beta = \mathbf{1}_m, p_{it} = 1$, and set $\tilde{\eta}_{it} = \log \frac{p_{it}}{1-p_{it}} + \frac{y_{it}-p_{it}}{p_{it}(1-p_{it})}$ for each i and t .
- 2: **repeat**
- 3: **repeat**
- 4: Set \mathbf{W} as an $N \times N$ diagonal matrix with diagonal elements $W_{it} = p_{it}(1 - p_{it})$
- 5: Set $\mathbf{V} = \mathbf{W}^{-1} + \sigma^2(\mathbf{R}_\theta \otimes \mathbf{I}_T)$
- 6: Update $\beta = (\mathbf{X}' \mathbf{V}^{-1} \mathbf{X})^{-1} \mathbf{X}' \mathbf{V}^{-1} \tilde{\eta}$

- 7: Set $\mathbf{Z} = \sigma^2(\mathbf{R}_\theta \otimes I_T) \mathbf{V}^{-1}(\tilde{\boldsymbol{\eta}} - \mathbf{X}' \boldsymbol{\beta})$
- 8: Update $p_{it} = \left(\frac{\exp\{\mathbf{X}' \boldsymbol{\beta} + \mathbf{Z}\}}{1_N + \exp\{\mathbf{X}' \boldsymbol{\beta} + \mathbf{Z}\}} \right)_{it}$ and $\tilde{\eta}_{it} = \log \frac{p_{it}}{1-p_{it}} + \frac{y_{it}-p_{it}}{p_{it}(1-p_{it})}$ for each i and t
- 9: **until** $\{\tilde{\eta}_{it}\}_{it}$ converges
- 10: Update $\boldsymbol{\omega} = \arg \min_{\boldsymbol{\omega}} L(\boldsymbol{\omega})$, where $L(\boldsymbol{\omega})$ is the negative log-likelihood function (12)
- 11: Update $(\sigma^2, \boldsymbol{\theta}) = \boldsymbol{\omega}$
- 12: **until** $\boldsymbol{\beta}$ and $\boldsymbol{\omega}$ converge
- 13: Return $\boldsymbol{\beta}$ and $\boldsymbol{\omega}$

B Assumptions

1. The parameter $\boldsymbol{\beta}$ belongs to an open set $B \subseteq \mathbb{R}^m$ and the parameter $\boldsymbol{\omega}$ belongs to an open set $\Omega \subseteq \mathbb{R}^{d+1}$.
2. The model matrix X_{it} lies almost surely in a nonrandom compact subset of \mathbb{R}^m such that $Pr(\sum_{i=1}^n \sum_{t=1}^T X'_{it} X_{it} > 0) = 1$.

For any matrix A , define $\|A\| \equiv \sqrt{\text{tr}(A'A)}$; for the covariance matrix $\mathbf{V}(\boldsymbol{\omega})$, define $V_i(\boldsymbol{\omega}) \equiv \partial \mathbf{V}(\boldsymbol{\omega}) / \partial \omega_i$ and $V_{ij}(\boldsymbol{\omega}) \equiv \partial \mathbf{V}(\boldsymbol{\omega}) / \partial \omega_i \partial \omega_j$; for $\boldsymbol{\omega} \in \Omega$, denote \xrightarrow{u} as uniform convergence of nonrandom functions over compact subsets of Ω .

3. $J_N(\boldsymbol{\omega}) P_N(\boldsymbol{\omega})^{-1} \xrightarrow{d} W(\boldsymbol{\omega})$ for some nonsingular $W(\boldsymbol{\omega})$, which is continuous in $\boldsymbol{\omega}$, where $P_N(\boldsymbol{\omega}) = \text{diag}(\|\Pi(\boldsymbol{\omega}) V_1(\boldsymbol{\omega})\|, \dots, \|\Pi(\boldsymbol{\omega}) V_{d+1}(\boldsymbol{\omega})\|)$ and $\Pi(\boldsymbol{\omega}) = \mathbf{V}(\boldsymbol{\omega})^{-1} - \mathbf{V}(\boldsymbol{\omega})^{-1} \mathbf{X} (\mathbf{X}' \mathbf{V}(\boldsymbol{\omega})^{-1} \mathbf{X})^{-1} \mathbf{X}' \mathbf{V}(\boldsymbol{\omega})^{-1}$.
4. If there exists a sequence $\{r_N\}_{N \geq 1}$ with $\limsup_{N \rightarrow \infty} r_N/N \leq 1 - \delta$, for some $\delta \in (0, 1)$, such that for any compact subset $K \subseteq \Omega$, there exist constants $0 < C_1(K) < \infty$ and

$C_2(K) > 0$ such that

$$\lim \sup_{N \rightarrow \infty} \max\{|\lambda_N|, |\lambda_N^i|, |\lambda_N^{ij}| : 1 \leq i, j \leq k\} < C_1(K) < \infty$$

and

$$\lim \sup_{N \rightarrow \infty} \min\{|\lambda_1|, |\lambda_{r_N}^i| : 1 \leq i \leq k\} > C_2(K) > 0,$$

uniformly in $\omega \in K$, where $|\lambda_1| \leq \dots \leq |\lambda_N|$ are the absolute eigenvalues of $\mathbf{V}(\omega)$, $|\lambda_1^i| \leq \dots \leq |\lambda_N^i|$ are the absolute eigenvalues of $V_i(\omega)$, and $|\lambda_1^{ij}| \leq \dots \leq |\lambda_N^{ij}|$ are the absolute eigenvalues of $V_{ij}(\omega)$.

Assumption 2 holds when the row vectors of \mathbf{X} are linear independent. Thus, if only the linear effect is considered in the mean function, then orthogonal designs or orthogonal array-based designs, such as OA-based Latin hypercube designs (Tang, 1993), can be chosen for sampling schemes. The conditions for Assumption 4 can be referred to Cressie and Lahiri (1996), in which the checkable conditions for rectangular lattice of data sites and irregularly located data sites are given. For instance, for rectangular lattice of data sites, with certain correlation functions, a sufficient condition is choosing data locations whose minimum distance is sufficiently large. More details can be seen in Cressie and Lahiri (1996). Thus, space-filling designs, such as Latin hypercube designs (McKay et al., 1979) and maximin distance designs (Johnson et al., 1990), can be chosen for sampling schemes.

C Proof of Theorem 3.1

The model (4) can be seen as a binary time series model with random effects by multiplying an identity matrix on \mathbf{Z} , that is,

$$\text{logit}(\mathbf{p}) = \mathbf{X}\boldsymbol{\beta} + I_N \mathbf{Z}, \quad \mathbf{Z} \sim \mathcal{N}(\mathbf{0}_N, \Sigma(\boldsymbol{\omega})),$$

where I_N and \mathbf{Z} are viewed as the model matrix and coefficients of random effects, respectively. Therefore, if the variance-covariance parameters are given, inference of $\boldsymbol{\beta}$ is a special case of the binary time series model with random effects in Hung et al. (2008). Therefore, following Theorem 1 in Hung et al. (2008), the score function $S_N(\boldsymbol{\beta}, \boldsymbol{\omega})$ is asymptotically normally distributed.

D Proof of Theorem 3.3

According to Breslow and Clayton (1993), one can view the inference on the variance-variance component as an iterative procedure for the linear mixed model

$$\tilde{\boldsymbol{\eta}} = \mathbf{X}\boldsymbol{\beta} + I_N \mathbf{Z} + \boldsymbol{\epsilon}, \quad \boldsymbol{\epsilon} \sim \mathcal{N}(\mathbf{0}_N, \mathbf{W}^{-1})$$

with the iterative weight \mathbf{W}^{-1} . Thus, it is a special case of the Gaussian general linear model in Cressie and Lahiri (1993) with response vector $\tilde{\boldsymbol{\eta}}$ and variance-covariance component $\Sigma(\boldsymbol{\omega}) + \mathbf{W}^{-1}$ with parameters $\boldsymbol{\omega}$. Since the asymptotic distribution of REML estimators for the variance-covariance parameters has been shown in Cressie and Lahiri (1993) for a Gaussian general linear model, the result directly follows as a special case of Corollary 3.3 in Cressie and Lahiri (1993). Note that Assumption 4 in Appendix B implies the conditions

for Corollary 3.3 in Cressie and Lahiri (1993). See the proof of Theorem 2.2 in Cressie and Lahiri (1996).

E Proof of Lemma 4.1

We start the proof by deriving the conditional distribution from a simple model (1) (without time-series), and then extend the result to prove Lemma 4.1. First, a definition and a lemma about multivariate log-normal distribution are in order.

Definition E.1. Suppose $\boldsymbol{\xi} = (\xi_1, \dots, \xi_n)'$ has a multivariate normal distribution with mean $\boldsymbol{\mu}_n$ and covariance variance $\boldsymbol{\Sigma}_{n \times n}$. Then $\mathbf{b} = \exp\{\boldsymbol{\xi}\}$ has a *multivariate log-normal distribution*. Denote it as $\mathbf{b} \sim \mathcal{LN}(\boldsymbol{\mu}_n, \boldsymbol{\Sigma}_{n \times n})$.

Lemma E.1. Suppose \mathbf{b}^n and b_{n+1} have a multivariate log-normal distribution

$$\begin{pmatrix} \mathbf{b}^n \\ b_{n+1} \end{pmatrix} \sim \mathcal{LN} \left(\begin{pmatrix} \boldsymbol{\mu}^n \\ \mu_{n+1} \end{pmatrix}, \begin{bmatrix} \boldsymbol{\Sigma}_{n \times n} & \mathbf{r} \\ \mathbf{r}' & \sigma_{n+1}^2 \end{bmatrix} \right).$$

The conditional distribution of b_{n+1} given \mathbf{b}^n is $b_{n+1} | \mathbf{b}^n \sim \mathcal{LN}(\mu^*, v^*)$, where $\mu^* = \mu_{n+1} + \mathbf{r}' \boldsymbol{\Sigma}_{n \times n}^{-1} (\log \mathbf{b}^n - \boldsymbol{\mu}^n)$ and $v^* = \sigma_{n+1}^2 - \mathbf{r}' \boldsymbol{\Sigma}_{n \times n}^{-1} \mathbf{r}$.

Proof. Using transformation of a standard normal distribution, one can show that the joint probability density function of the multivariate log-normal distribution \mathbf{b}^n is

$$g_{\mathbf{b}^n}(b_1, \dots, b_n) = \frac{1}{(2\pi)^{n/2} |\boldsymbol{\Sigma}_{n \times n}|^{1/2}} \frac{1}{\prod_{i=1}^n b_i} \exp\left\{-\frac{1}{2} (\log \mathbf{b}^n - \boldsymbol{\mu}_n)' \boldsymbol{\Sigma}_{n \times n}^{-1} (\log \mathbf{b}^n - \boldsymbol{\mu}_n)\right\}.$$

Denote $\mathbf{b}^{n+1} = (b_1, \dots, b_n, b_{n+1})$, $\boldsymbol{\mu}^{n+1} = (\mu_1, \dots, \mu_n, \mu_{n+1})$ and

$$\boldsymbol{\Sigma}_{(n+1) \times (n+1)} = \begin{bmatrix} \boldsymbol{\Sigma}_{n \times n} & \mathbf{r} \\ \mathbf{r}' & \sigma_{n+1} \end{bmatrix}.$$

Then, the conditional probability density function of b_{n+1} given \mathbf{b}^n can be derived as

$$\begin{aligned} g_{b_{n+1}|\mathbf{b}^n}(b_{n+1}|\mathbf{b}^n) &\propto g(b_1, \dots, b_n, b_{n+1}) \\ &\propto \frac{1}{b_{n+1}} \exp\left\{-\frac{1}{2} (\log \mathbf{b}^{n+1} - \boldsymbol{\mu}_{n+1})' \boldsymbol{\Sigma}_{(n+1) \times (n+1)}^{-1} (\log \mathbf{b}^{n+1} - \boldsymbol{\mu}_{n+1})\right\}. \end{aligned}$$

Let $\mathbf{a}_1 = \log \mathbf{b}^n - \boldsymbol{\mu}^n$ and $\mathbf{a}_2 = \log b^{n+1} - \mu^{n+1}$. Applying the partitioned matrix inverse results (page 99 of Harville (1997)) gives

$$\begin{aligned} &(\log \mathbf{b}^{n+1} - \boldsymbol{\mu}^{n+1})' \boldsymbol{\Sigma}_{(n+1) \times (n+1)}^{-1} (\log \mathbf{b}^{n+1} - \boldsymbol{\mu}^{n+1}) \\ &= \begin{bmatrix} \mathbf{a}'_1 & \mathbf{a}'_2 \end{bmatrix} \begin{bmatrix} \boldsymbol{\Sigma}_{n \times n} & \mathbf{r} \\ \mathbf{r}' & \sigma_{n+1} \end{bmatrix}^{-1} \begin{bmatrix} \mathbf{a}_1 \\ \mathbf{a}_2 \end{bmatrix} \\ &= (\mathbf{a}_2 - \mathbf{r}' \boldsymbol{\Sigma}_{n \times n}^{-1} \mathbf{a}_1)' \sigma_{22 \cdot 1}^{-1} (\mathbf{a}_2 - \mathbf{r}' \boldsymbol{\Sigma}_{n \times n}^{-1} \mathbf{a}_1) + \mathbf{a}'_1 \boldsymbol{\Sigma}_{n \times n}^{-1} \mathbf{a}_1 \\ &= (\mathbf{a}_2 - \mathbf{r}' \boldsymbol{\Sigma}_{n \times n}^{-1} \mathbf{a}_1)^2 / \sigma_{22 \cdot 1} + \mathbf{a}'_1 \boldsymbol{\Sigma}_{n \times n}^{-1} \mathbf{a}_1, \end{aligned}$$

where $\sigma_{22 \cdot 1} = \sigma_{n+1}^2 - \mathbf{r}' \boldsymbol{\Sigma}_{n \times n}^{-1} \mathbf{r}$ and is a real number.

Thus, the conditional probability density function of b_{n+1} given \mathbf{b}^n can be simplified as

$$\begin{aligned} g_{b_{n+1}|\mathbf{b}^n}(b_{n+1}|\mathbf{b}^n) &\propto \frac{1}{b_{n+1}} \exp\left\{-\frac{1}{2\sigma_{22.1}}(\mathbf{a}_2 - \mathbf{r}'\Sigma_{n\times n}^{-1}\mathbf{a}_1)^2 - \frac{1}{2}\mathbf{a}_1'\Sigma_{n\times n}^{-1}\mathbf{a}_1\right\} \\ &\propto \frac{1}{b_{n+1}} \exp\left\{-\frac{1}{2\sigma_{22.1}}(\mathbf{a}_2 - \mathbf{r}'\Sigma_{n\times n}^{-1}\mathbf{a}_1)^2\right\} \\ &= \frac{1}{b_{n+1}} \exp\left\{-\frac{1}{2\sigma_{22.1}}\left(\log b_{n+1} - (\mu_{n+1} + \mathbf{r}'\Sigma_{n\times n}^{-1}(\log \mathbf{b}^n - \boldsymbol{\mu}^n))\right)^2\right\}. \end{aligned}$$

Therefore, according to the probability density function of a log-normal distribution, we have $b_{n+1}|\mathbf{b}^n \sim \mathcal{LN}(\mu^*, v^*)$, where $\mu^* = \mu_{n+1} + \mathbf{r}'\Sigma_{n\times n}^{-1}(\log \mathbf{b}^n - \boldsymbol{\mu}^n)$ and $v^* = \sigma_{22.1}^2 = \sigma_{n+1}^2 - \mathbf{r}'\Sigma_{n\times n}^{-1}\mathbf{r}$. \square

Lemma E.2. Consider the model (1) (without time-series), given $(p(\mathbf{x}_1), \dots, p(\mathbf{x}_n))' = \mathbf{p}^n$, the conditional distribution of $p(\mathbf{x}_{n+1})$ is a logit-normal distribution, that is, $p(\mathbf{x}_{n+1})|\mathbf{p}^n \sim \text{Logitnormal}(m(\mathbf{p}^n), v(\mathbf{p}^n))$ with

$$m(\mathbf{p}^n) = \mu(\mathbf{x}_{n+1}) + \mathbf{r}'_{\boldsymbol{\theta}} \mathbf{R}_{\boldsymbol{\theta}}^{-1} (\log \frac{\mathbf{p}^n}{\mathbf{1} - \mathbf{p}^n} - \boldsymbol{\mu}^n) \quad \text{and} \quad v(\mathbf{p}^n) = \sigma^2 (1 - \mathbf{r}'_{\boldsymbol{\theta}} \mathbf{R}_{\boldsymbol{\theta}}^{-1} \mathbf{r}_{\boldsymbol{\theta}}),$$

where $\boldsymbol{\mu}^n = (\mu(\mathbf{x}_1), \dots, \mu(\mathbf{x}_n))'$, $\mu(\mathbf{x}_i) = \alpha_0 + \mathbf{x}'_i \boldsymbol{\alpha}$, $\mathbf{r}_{\boldsymbol{\theta}} = (R_{\boldsymbol{\theta}}(\mathbf{x}_{n+1}, \mathbf{x}_1), \dots, R_{\boldsymbol{\theta}}(\mathbf{x}_{n+1}, \mathbf{x}_n))'$, and $\mathbf{R}_{\boldsymbol{\theta}} = \{R_{\boldsymbol{\theta}}(\mathbf{x}_i, \mathbf{x}_j)\}$.

Proof. Let $\eta_i = \mu(\mathbf{x}_i) + Z(\mathbf{x}_i)$ and $b_i = \exp\{\eta_i\} = p(\mathbf{x}_i)/(1 - p(\mathbf{x}_i))$ for $i = 1, \dots, n+1$. Since $(\eta_1, \dots, \eta_n, \eta_{n+1})' \sim \mathcal{N}(\boldsymbol{\mu}^{n+1}, \sigma^2 \mathbf{R}_{\boldsymbol{\theta}}^*)$, where $\boldsymbol{\mu}^{n+1} = ((\boldsymbol{\mu}^n)', \mu(\mathbf{x}_{n+1}))'$ and

$$\mathbf{R}_{\boldsymbol{\theta}}^* = \begin{bmatrix} \mathbf{R}_{\boldsymbol{\theta}} & \mathbf{r}_{\boldsymbol{\theta}} \\ \mathbf{r}'_{\boldsymbol{\theta}} & 1 \end{bmatrix},$$

we have $(b_1, \dots, b_n, b_{n+1})' \sim \mathcal{LN}(\boldsymbol{\mu}^{n+1}, \sigma^2 \mathbf{R}_{\boldsymbol{\theta}}^*)$ by Definition E.1. Thus, using Jacobian of

the transformation and Lemma E.1, we have

$$\begin{aligned}
& g_{p(\mathbf{x}_{n+1})|p(\mathbf{x}_1), \dots, p(\mathbf{x}_n)}(p_{n+1}|p_1, \dots, p_n) \\
&= g_{b_{n+1}|b_1, \dots, b_n}(\frac{p_{n+1}}{1-p_{n+1}} | \frac{p_1}{1-p_1}, \dots, \frac{p_n}{1-p_n}) \frac{1}{(1-p_{n+1})^2} \\
&\propto \frac{1-p_{n+1}}{p_{n+1}} \exp\left\{-\frac{\left(\log \frac{p_{n+1}}{1-p_{n+1}} - (\mu(\mathbf{x}_{n+1}) + \mathbf{r}'_{\theta} \mathbf{R}_{\theta}^{-1} (\log \frac{\mathbf{p}^n}{1-\mathbf{p}^n} - \boldsymbol{\mu}^n))\right)^2}{2\sigma^2(1 - \mathbf{r}'_{\theta} \mathbf{R}_{\theta}^{-1} \mathbf{r}_{\theta})}\right\} \frac{1}{(1-p_{n+1})^2} \\
&\propto \frac{1}{p_{n+1}(1-p_{n+1})} \exp\left\{-\frac{\left(\log \frac{p_{n+1}}{1-p_{n+1}} - (\mu(\mathbf{x}_{n+1}) + \mathbf{r}'_{\theta} \mathbf{R}_{\theta}^{-1} (\log \frac{\mathbf{p}^n}{1-\mathbf{p}^n} - \boldsymbol{\mu}^n))\right)^2}{2\sigma^2(1 - \mathbf{r}'_{\theta} \mathbf{R}_{\theta}^{-1} \mathbf{r}_{\theta})}\right\}.
\end{aligned}$$

Therefore, according to the probability density function of a logit-normal distribution, we have $p(\mathbf{x}_{n+1})|\mathbf{p}^n \sim \text{Logitnormal}(m(\mathbf{p}^n), v(\mathbf{p}^n))$. \square

Similarly, the result of Lemma E.2 can be extended to the general model (3). Given $\mathbf{Y} = (\mathbf{y}'_1, \dots, \mathbf{y}'_T, y_{n+1,1}, \dots, y_{n+1,s-1})'$, at a fixed time-step s , $p_s(\mathbf{x}_i)$ can be seen to have the model (1) with mean function $\mu(\mathbf{x}_i, \mathbf{Y}) = \sum_{r=1}^R \varphi_r y_{i,s-r} + \alpha_0 + \mathbf{x}'_i \boldsymbol{\alpha} + \sum_{l=1}^L \boldsymbol{\gamma}_l \mathbf{x}_i y_{i,s-l}$. Thus, by Lemma E.2, denote $\mathbf{p}_s = (p_s(\mathbf{x}_1), \dots, p_s(\mathbf{x}_n))'$, we have

$$p_s(\mathbf{x}_{n+1})|\mathbf{p}_s, \mathbf{Y} \sim \text{Logitnormal}(m(\mathbf{p}_s, \mathbf{Y}), v(\mathbf{p}_s, \mathbf{Y})),$$

where $m(\mathbf{p}_s, \mathbf{Y}) = \mu(\mathbf{x}_{n+1}, \mathbf{Y}) + \mathbf{r}'_{\theta} \mathbf{R}_{\theta}^{-1} (\log \frac{\mathbf{p}_s}{1-\mathbf{p}_s} - \boldsymbol{\mu}^n)$, $\boldsymbol{\mu}^n = (\mu(\mathbf{x}_1, \mathbf{Y}), \dots, \mu(\mathbf{x}_n, \mathbf{Y}))'$, and $v(\mathbf{p}_s, \mathbf{Y}) = \sigma^2(1 - \mathbf{r}'_{\theta} \mathbf{R}_{\theta}^{-1} \mathbf{r}_{\theta})$. By the fact that $Z_t(\mathbf{x})$ is independent over time, which implies $p_s(\mathbf{x})$ is independent of $p_t(\mathbf{x})$ for any $t \neq s$, $p_s(\mathbf{x}_{n+1})|D_{n+1,s}$ and $p_s(\mathbf{x}_{n+1})|\mathbf{p}_s, \mathbf{Y}$ have the same distribution. So, $p_s(\mathbf{x}_{n+1})|D_{n+1,s} \sim \text{Logitnormal}(m(D_{n+1,s}), v(D_{n+1,s}))$, where $m(D_{n+1,s}) = m(\mathbf{p}_s, \mathbf{Y})$ and $v(D_{n+1,s}) = v(\mathbf{p}_s, \mathbf{Y})$.

F Proof of Theorem 4.3

(i) First, one can show that if $(p_s(\mathbf{x}_{n+1}), D_{n+1,s})$ has a joint distribution for which the conditional mean of $p_s(\mathbf{x}_{n+1})$ given $D_{n+1,s}$ exists, then $\mathbb{E}[p(\mathbf{x}_{n+1})|D_{n+1,s}]$ is the minimum mean squared error predictor of $p(\mathbf{x}_{n+1})$. See Theorem 3.2.1 in Santner et al. (2003). Thus, by the result of Lemma 4.1, we have the conditional mean $\mathbb{E}[p(\mathbf{x}_{n+1})|D_{n+1,s}] = \kappa(m(D_{n+1,s}), v(D_{n+1,s}))$ with variance $\mathbb{V}[p(\mathbf{x}_{n+1})|D_{n+1,s}] = \tau(m(D_{n+1,s}), v(D_{n+1,s}))$.

(ii) If $\mathbf{x}_{n+1} = \mathbf{x}_i$ for $i = 1, \dots, n$, then $m(D_{n+1,s}) = \log(p_s(\mathbf{x}_i)/(1-p_s(\mathbf{x}_i)))$ and $v(D_{n+1,s}) = 0$, which implies that

$$\kappa(m(D_{n+1,s}), 0) = \exp\{m(D_{n+1,s})\}/(1 + \exp\{m(D_{n+1,s})\}) = p_s(\mathbf{x}_i)$$

and $\tau(m(D_{n+1,s}), 0) = 0$ by using transformation of a normal distribution. Thus, by Theorem 4.3 (i), we have $\mathbb{E}[p_s(\mathbf{x}_{n+1})|D_{n+1,s}] = p_s(\mathbf{x}_i)$ and $\mathbb{V}[p_s(\mathbf{x}_{n+1})|D_{n+1,s}] = 0$.

(iii) Let $X \sim \mathcal{N}(m(D_{n+1,s}), v(D_{n+1,s}))$, $P = \exp\{X\}/(1 + \exp\{X\})$, which has the distribution *Logitnormal*($m(D_{n+1,s}), v(D_{n+1,s})$), and $Q(q; D_{n+1,s})$ be the q -th quantile of P . Consider the function $f(x) = \log(x/(1-x))$. The derivative is $f'(x) = 1/(x(1-x))$. Thus, for $0 < x < 1$ the derivative is positive and the $f(x)$ function is increasing in x . Then,

$$\begin{aligned} & \Pr\{P > Q(q; D_{n+1,s})\} = q \\ \Leftrightarrow & \Pr\left\{\frac{\exp\{X\}}{1 + \exp\{X\}} > Q(q; D_{n+1,s})\right\} = q \\ \Leftrightarrow & \Pr\left\{f\left(\frac{\exp\{X\}}{1 + \exp\{X\}}\right) > f(Q(q; D_{n+1,s}))\right\} = q \\ \Leftrightarrow & \Pr\left\{X > \log \frac{Q(q; D_{n+1,s})}{1 - Q(q; D_{n+1,s})}\right\} = q \end{aligned}$$

$$\begin{aligned}
&\Leftrightarrow \Pr \left\{ \frac{X - m(D_{n+1,s})}{\sqrt{v(D_{n+1,s})}} > \frac{1}{\sqrt{v(D_{n+1,s})}} \left(\log \frac{Q(q; D_{n+1,s})}{1 - Q(q; D_{n+1,s})} - m(D_{n+1,s}) \right) \right\} = q \\
&\Leftrightarrow \frac{1}{\sqrt{v(D_{n+1,s})}} \left(\log \frac{Q(q; D_{n+1,s})}{1 - Q(q; D_{n+1,s})} - m(D_{n+1,s}) \right) = z_q \\
&\Leftrightarrow Q(q; D_{n+1,s}) = \frac{\exp\{m(D_{n+1,s}) + z_q \sqrt{v(D_{n+1,s})}\}}{1 + \exp\{m(D_{n+1,s}) + z_q \sqrt{v(D_{n+1,s})}\}}.
\end{aligned}$$

G Algorithm: Metropolis-Hastings Algorithm

```

1: for  $j = 1$  to  $J$  do
2:   Set  $N_s = nT + s - 1$ .
3:   Start with a zero vector  $\mathbf{p}$  of size  $N_s$ .
4:   for  $k = 1$  to  $N_s$  do
5:     Generate a random value  $p_k^*$  from  $\text{Logitnormal}(m(\mathbf{p}_{-k}, \mathbf{y}_{-k}), v(\mathbf{p}_{-k}, \mathbf{y}_{-k}))$ .
6:     Generate an uniform random variable  $U \sim \text{Unif}(0, 1)$ .
7:     if  $U < \min\{1, \frac{f(y_k|p_k^*)}{f(y_k|p_k)}\}$  then
8:       Set  $\mathbf{p} = (p_1, \dots, p_k^*, \dots, p_{N_s})$ .
9:   Set  $\mathbf{p}^{(j)} = \mathbf{p}$ 
10:  Return  $\{\mathbf{p}^{(j)}\}_{j=1, \dots, J}$ .

```

In the algorithm, we first sample a value for the k -th component p_k from the conditional distribution of p_k given $p_j, y_j, j \neq k$, which is $\text{Logitnormal}(m(\mathbf{p}_{-k}, \mathbf{y}_{-k}), v(\mathbf{p}_{-k}, \mathbf{y}_{-k}))$, where

$$m(\mathbf{p}_{-k}, \mathbf{y}_{-k}) = \mu_t(\mathbf{x}_i) - \sum_{k \neq j} \frac{Q_{kj}}{Q_{kk}} \left(\log \frac{p_k}{1 - p_k} - \mu_t(\mathbf{x}_i) \right), \quad v(\mathbf{p}_{-k}, \mathbf{y}_{-k}) = \frac{\sigma^2}{Q_{kk}},$$

in which $\mu_t(\mathbf{x}_i) = \sum_{r=1}^R \varphi_r y_{i,t-r} + \mathbf{x}'_i \boldsymbol{\alpha} + \sum_{l=1}^L \boldsymbol{\gamma}_l \mathbf{x}_i y_{i,t-l}$ and Q_{kj} is the (k, j) -element of $\mathbf{R}_{\boldsymbol{\theta}}^{-1}$. Similar to Zhang (2002), we use the single-component MH algorithm, that is, to update only

a single component at each iteration. Moreover, the proposed distribution $f(p_k)$ is used for the single MH algorithm, so that the probability of accepting a new p_k^* is the minimum of 1 and $\frac{f(p_k^*|y_k)f(p_k)}{f(p_k|y_k)f(p_k^*)} \left(= \frac{f(y_k|p_k^*)}{f(y_k|p_k)} \right)$.

H Algorithm: Dynamic Binary Emulator

- 1: **for** $j = 1$ to J **do**
- 2: Set $N = nT$.
- 3: Start with a zero vector \mathbf{p} of size N .
- 4: **for** $i = 1$ to N **do**
- 5: Generate a random value p_k^* from $\text{Logitnormal}(m(\mathbf{p}_{-k}, \mathbf{y}_{-k}), v(\mathbf{p}_{-k}, \mathbf{y}_{-k}))$.
- 6: Generate an uniform random variable $U \sim \text{Unif}(0, 1)$.
- 7: **if** $U < \min\{1, \frac{f(y_k|p_k^*)}{f(y_k|p_k)}\}$ **then**
- 8: Set $\mathbf{p} = (p_1, \dots, p_k^*, \dots, p_N)$.
- 9: Set $\mathbf{p}_{n+1} = \mathbf{p}$, $\mathbf{Y}_{n+1} = \mathbf{Y}$, zero vectors \mathbf{p}_{new} and \mathbf{y}_{new} of size T .
- 10: **for** $t = 1$ to T **do**
- 11: Given $D_{n+1,t} = \{\mathbf{p}_{n+1}, \mathbf{Y}_{n+1}\}$, draw a sample $p_t(\mathbf{x}_{n+1})$ from $\text{Logitnormal}(m(D_{n+1,t}), v(D_{n+1,t}))$, and then draw a sample $y_t(\mathbf{x}_{n+1})$ from a Bernoulli distribution with parameter $p_t(\mathbf{x}_{n+1})$.
- 12: Update $\mathbf{p}_{n+1} = (\mathbf{p}'_{n+1}, p_t(\mathbf{x}_{n+1}))'$, $\mathbf{Y}_{n+1} = (\mathbf{Y}'_{n+1}, y_t(\mathbf{x}_{n+1}))'$, $(\mathbf{p}_{\text{new}})_t = p_t(\mathbf{x}_{n+1})$, and $(\mathbf{y}_{\text{new}})_t = y_t(\mathbf{x}_{n+1})$.
- 13: Set $\mathbf{p}_{\text{new}}^{(j)} = \mathbf{p}_{\text{new}}$ and $\mathbf{y}_{\text{new}}^{(j)} = \mathbf{y}_{\text{new}}$.
- 14: Take pointwise median from $\{\mathbf{p}_{\text{new}}^{(j)}\}_{j=1,\dots,J}$ and $\{\mathbf{y}_{\text{new}}^{(j)}\}_{j=1,\dots,J}$.

References

Atchison, J. and Shen, S. M. (1980). Logistic-normal distributions: some properties and uses. *Biometrika*, 67(2):261–272.

Barndorff-Nielsen, O. E. and Cox, D. R. (1997). *Asymptotic Techniques for Use in Statistics*. London: Chapman & Hall.

Breslow, N. E. and Clayton, D. G. (1993). Approximate inference in generalized linear mixed models. *Journal of the American statistical Association*, 88(421):9–25.

Conti, S. and O'Hagan, A. (2010). Bayesian emulation of complex multi-output and dynamic computer models. *Journal of Statistical Planning and Inference*, 140(3):640–651.

Cox, D. R. (1972). Regression models and life-tables. *Journal of the Royal Statistical Society, Series B*, 34(2):187–220.

Cox, D. R. (1975). Partial likelihood. *Biometrika*, 62(2):269–276.

Cressie, N. and Lahiri, S. N. (1993). The asymptotic distribution of reml estimators. *Journal of Multivariate Analysis*, 45(2):217–233.

Cressie, N. and Lahiri, S. N. (1996). Asymptotics for reml estimation of spatial covariance parameters. *Journal of Statistical Planning and Inference*, 50(3):327–341.

Frederic, P. and Lad, F. (2008). Two moments of the logitnormal distribution. *Communications in Statistics Simulation and Computation*, 37(7):1263–1269.

Fricker, T. E., Oakley, J. E., and Urban, N. M. (2013). Multivariate gaussian process emulators with nonseparable covariance structures. *Technometrics*, 55(1):47–56.

Friedman, J. H. (1991). Multivariate adaptive regression splines. *The Annals of Statistics*, 19(1):1–67.

Gelfand, A. E., Schmidt, A. M., Banerjee, S., and Sirmans, C. (2004). Nonstationary multivariate process modeling through spatially varying coregionalization. *Test*, 13(2):263–312.

Gramacy, R. B. and Apley, D. W. (2015). Local gaussian process approximation for large computer experiments. *Journal of Computational and Graphical Statistics*, 24(2):561–578.

Gramacy, R. B., Bingham, D., Holloway, J. P., Grosskopf, M. J., Kuranz, C. C., Rutter, E., Trantham, M., and Drake, R. P. (2015). Calibrating a large computer experiment simulating radiative shock hydrodynamics. *The Annals of Applied Statistics*, 9(3):1141–1168.

Gramacy, R. B. and Polson, N. G. (2011). Particle learning of gaussian process models for sequential design and optimization. *Journal of Computational and Graphical Statistics*, 20(1):102–118.

Harville, D. A. (1974). Bayesian inference for variance components using only error contrasts. *Biometrika*, 61(2):383–385.

Harville, D. A. (1977). Maximum likelihood approaches to variance component estimation and to related problems. *Journal of the American Statistical Association*, 72(358):320–338.

Harville, D. A. (1997). *Matrix Algebra from a Statistician’s Perspective*, volume 157. Springer.

Hodges, J. S. and Reich, B. J. (2010). Adding spatially-correlated errors can mess up the fixed effect you love. *The American Statistician*, 64(4):325–334.

Huang, J., Zarnitsyna, V. I., Liu, B., Edwards, L. J., Jiang, N., Evavold, B. D., and Zhu, C. (2010). The kinetics of two-dimensional tcr and pmhc interactions determine t-cell responsiveness. *Nature*, 464(7290):932–936.

Hung, Y., Zarnitsyna, V., Zhang, Y., Zhu, C., and Wu, C. F. J. (2008). Binary time series modeling with application to adhesion frequency experiments. *Journal of the American Statistical Association*, 103(483).

Johnson, M. E., Moore, L. M., and Ylvisaker, D. (1990). Minimax and maximin distance designs. *Journal of Statistical Planning and Inference*, 26(2):131–148.

Karatzoglou, A., Smola, A., Hornik, K., and Zeileis, A. (2004). kernlab – an S4 package for kernel methods in R. *Journal of Statistical Software*, 11(9):1–20.

Kennedy, M. C. and O’Hagan, A. (2001). Bayesian calibration of computer models (with discussion). *Journal of the Royal Statistical Society: Series B*, 63(3):425–464.

Li, R. and Sudjianto, A. (2005). Analysis of computer experiments using penalized likelihood in gaussian kriging models. *Technometrics*, 47(2):111–120.

Liu, F. and West, M. (2009). A dynamic modelling strategy for bayesian computer model emulation. *Bayesian Analysis*, 4(2):393–411.

McKay, M. D., Beckman, R. J., and Conover, W. J. (1979). Comparison of three methods for selecting values of input variables in the analysis of output from a computer code. *Technometrics*, 21(2):239–245.

Mead, R. (1965). A generalised logit-normal distribution. *Biometrics*, 21(3):721–732.

Nickisch, H. and Rasmussen, C. E. (2008). Approximations for binary Gaussian process classification. *Journal of Machine Learning Research*, 9:2035–2078.

Paciorek, C. J. (2010). The importance of scale for spatial-confounding bias and precision of spatial regression estimators. *Statistical Science*, 25(1):107.

Patterson, H. D. and Thompson, R. (1971). Recovery of inter-block information when block sizes are unequal. *Biometrika*, 58(3):545–554.

Patterson, H. D. and Thompson, R. (1974). Maximum likelihood estimation of components of variance. In *Proceedings of the 8th International Biometric Conference*, pages 197–207. Biometric Society, Washington, DC.

Plumlee, M. and Joseph, V. R. (2018). Orthogonal gaussian process models. *Statistica Sinica*, to appear. arXiv preprint arXiv:1611.00203.

R Core Team (2015). *R: A Language and Environment for Statistical Computing*. R Foundation for Statistical Computing, Vienna, Austria.

Rasmussen, C. E. and Williams, C. K. I. (2006). *Gaussian Processes for Machine Learning*. the MIT Press.

Sacks, J., Welch, W. J., Mitchell, T. J., and Wynn, H. P. (1989). Design and analysis of computer experiments. *Statistical Scicence*, 4(4):409–423.

Santner, T. J., Williams, B. J., and Notz, W. I. (2003). *The Design and Analysis of Computer Experiments*. Springer New York.

Shi, J. Q. and Cheng, Y. (2014). *GPFDA: Apply Gaussian Process in Functional Data Analysis*. R package version 2.2.

Shi, J. Q. and Choi, T. (2011). *Gaussian Process Regression Analysis for Functional Data*. CRC Press.

Slud, E. and Kedem, B. (1994). Partial likelihood analysis of logistic regression and autoregression. *Statistica Sinica*, 4(1):89–106.

Sung, C.-L. (2017). *binaryGP: Fit and Predict a Gaussian Process Model with (Time-Series) Binary Response*. R package version 0.2.

Sung, C.-L., Gramacy, R. B., and Haaland, B. (2018). Potentially predictive variance reducing subsample locations in local gaussian process regression. *Statistica Sinica*, to appear. arXiv preprint arXiv:1604.04980.

Tang, B. (1993). Orthogonal array-based latin hypercubes. *Journal of the American Statistical Association*, 88(424):1392–1397.

Tuo, R. and Wu, C. F. J. (2015). Efficient calibration for imperfect computer models. *Annals of Statistics*, 43(6):2331–2352.

Wang, B. and Shi, J. Q. (2014). Generalized gaussian process regression model for non-gaussian functional data. *Journal of the American Statistical Association*, 109(507):1123–1133.

Williams, C. K. and Barber, D. (1998). Bayesian classification with gaussian processes. *IEEE Transactions on Pattern Analysis and Machine Intelligence*, 20(12):1342–1351.

Wutzler, T. (2012). *logitnorm: Functions for the logitnormal distribution*. R package version 0.8.29.

Zarnitsyna, V. I., Huang, J., Zhang, F., Chien, Y.-H., Leckband, D., and Zhu, C. (2007). Memory in receptor-ligand-mediated cell adhesion. *Proceedings of the National Academy of Science, U.S.A.*, 104(46):18037–18042.

Zeger, S. L. and Qaqish, B. (1988). Markov regression models for time series: a quasi-likelihood approach. *Biometrics*, 44(4):1019–1031.

Zhang, H. (2002). On estimation and prediction for spatial generalized linear mixed models. *Biometrics*, 58(1):129–136.